nature COMMUNICATIONS

ARTICLE

https://doi.org/10.1038/s41467-021-24250-1 OPEN

Climate pacing of millennial sea-level change variability in the central and western Mediterranean

Matteo Vacchi[1,2✉], Kristen M. Joyse[3], Robert E. Kopp[3], Nick Marriner[4], David Kaniewski[5] & Alessio Rovere[6]

Future warming in the Mediterranean is expected to significantly exceed global values with unpredictable implications on the sea-level rise rates in the coming decades. Here, we apply an empirical-Bayesian spatio-temporal statistical model to a dataset of 401 sea-level index points from the central and western Mediterranean and reconstruct rates of sea-level change for the past 10,000 years. We demonstrate that the mean rates of Mediterranean industrial-era sea-level rise have been significantly faster than any other period since ~4000 years ago. We further highlight a previously unrecognized variability in Mediterranean sea-level change rates. In the Common Era, this variability correlates with the occurrence of major regional-scale cooling/warming episodes. Our data show a sea-level stabilization during the Late Antique Little Ice Age cold event, which interrupted a general rising trend of ~0.45 mm a^{-1} that characterized the warming episodes of the Common Era. By contrast, the Little Ice Age cold event had only minor regional effects on Mediterranean sea-level change rates.

[1] Dipartimento di Scienze Della Terra, Università di Pisa, Pisa, Italy. [2] CIRSEC—Centro Interdipartimentale di Ricerca per lo Studio degli Effetti del Cambiamento climatico dell'Università di Pisa, Pisa, Italy. [3] Department of Earth & Planetary Sciences and Rutgers Institute of Earth, Ocean, and Atmospheric Sciences, Rutgers University, New Brunswick, NJ, USA. [4] CNRS, ThéMA, Université de Franche-Comté, UMR 6049, MSHE Ledoux, Besançon, Cedex, France. [5] TRACES, UMR 5608 CNRS, Université Toulouse Jean Jaurès, Maison de la Recherche, Toulouse, Cedex 9, France. [6] MARUM, Center for Marine Environmental Sciences, University of Bremen, Bremen, Germany. ✉email: matteo.vacchi@unipi.it

Climate and sea-level reconstructions for the pre-industrial period (i.e., before 1850 CE) provide context for current and future changes[1–3]. Determining the rates, mechanisms, and geographic variability of relative sea-level (RSL) change following the Last Glacial Maximum (LGM) is relevant to gauging how climatic forcing may influence the rates of future sea-level change[3,4]. Compilations of sea-level proxies have facilitated the quantification of the response of the solid Earth and geoid to ice-mass redistribution[5–7] and provided constraints for statistical and geophysical models used to project future sea-level rise[8]. The Mediterranean Sea is a semi-enclosed basin lying in a transition zone between mid-latitude and subtropical atmospheric circulation regimes and is characterized by strong land-sea contrasts[9]. For this reason, it is considered a hotspot of current climate change[9–11], and future warming in the Mediterranean area is expected to exceed global rates by ~25%[12]. This may result in high sea-level rise rates compared to global averages, leading to significant losses in the environmental, cultural and economic values of Mediterranean coasts[13]. Furthermore, semi-closed basins are poorly resolved by the ~1° resolution typical of global climate models included in CMIP5/6, which are generally used to drive projections of local dynamic sea-level change[14]. Finally, offset between data and glacio-isostatic adjustment (GIA) models were recently highlighted by extended sea-level records[15]. This adds complexity to defining the magnitude and spatial variability of the isostatic component, which affects both current and future sea-level changes.

The increasing availability of continuous and high-resolution Holocene and Common Era Mediterranean relative sea-level (RSL) reconstructions[15,16] provides the opportunity to explore the role of climatic factors in mediating sea-level variability in the Holocene (i.e., the last 11.7 ka). These data are of major importance because regional climatic forcing can lead to significant departures from global mean sea-level projections[10].

Here, we applied an empirical-Bayesian spatio-temporal statistical model[17] (see "Methods") to a dataset of 401 sea-level index points (SLIPs), defining the discrete position of past RSL in space and time[18]. We focus our analysis on the central and western Mediterranean (Fig. 1), which are less affected by neotectonic processes[19] than the eastern part. The results of our analysis constitute the first basin-scale assessment of sea-level variability in the Mediterranean for the last 10,000 years and represent the natural and geological backgrounds against which modern Mediterranean sea-level rise should be quantified.

Results and discussion

Millennial variability of sea-level change rates. The SLIPs database (Supplementary Table 1) is composed of (i) 391 radiocarbon-dated geological samples from transitional brackish environments, fossil intertidal bioconstructions, beachrocks, and (ii) 12 archeologically dated marine structures whose relationship with the contemporary mean sea-level is robustly defined[20]. The spatial distribution of the SLIPs covers a large portion of the central and northern sectors of the central and western Mediterranean basin, while in the southern sector the available data are restricted to the coasts of Malta and the Gulf of Gabes (Fig. 1). The SLIPs database allowed us to reconstruct the rates of RSL change in 48 sub-regions clustered according to their geographic proximity (Supplementary Fig. 1a). The average vertical accuracy of the different SLIPs is ±0.7 m (max ±1.3 m, min ±0.2 m) while the average age error is ±0.15 ka (max 0.62 ka, min 0.025 ka). All errors are reported at ±1σ. The age of the SLIPs spans the whole Holocene period (Supplementary Fig. 1b). 10.3% of the SLIPs date to the early Holocene (−10,000 to −6000 CE), 32.4% to the mid-Holocene (−6000 to −2000 CE), and 57.3% to the late Holocene (−2000 to 1950 CE). Virtually uncompressible samples (see "Methods") represent 36.5% of the entire record, while 39.4% of the SLIPs dates between −5000 and 1950 CE (Supplementary Fig. 1b).

The spatio-temporal model allowed us to reconstruct sea-level change rates since −8000 CE. There is a paucity of SLIPs for the

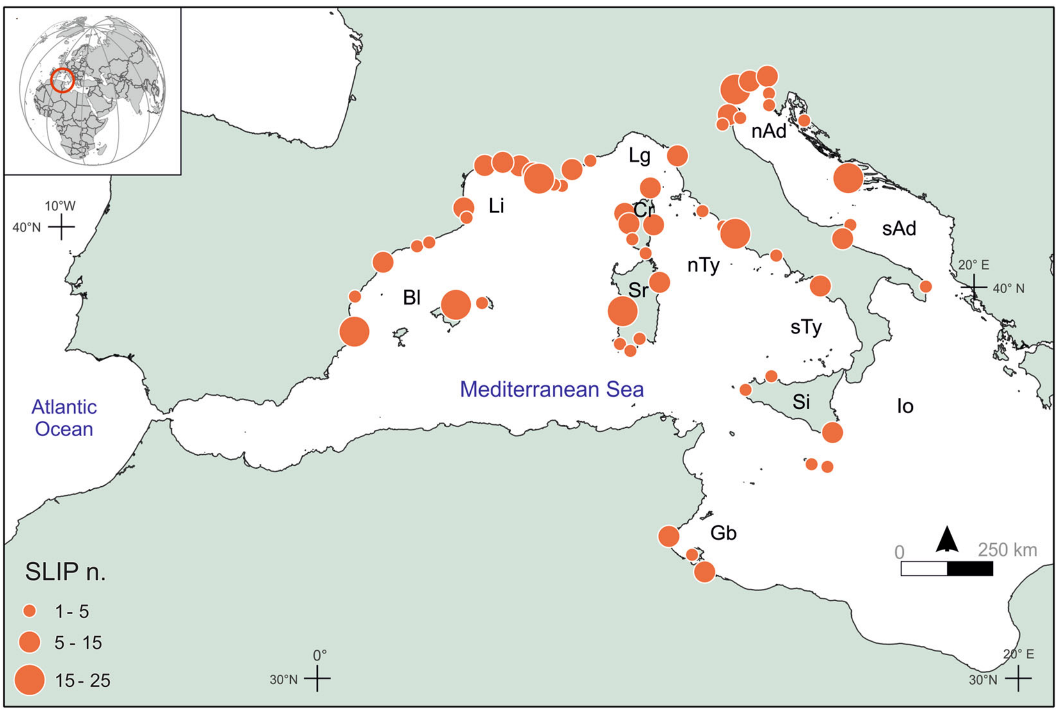

Fig. 1 Spatial distribution of the central and western Mediterranean sea-level index points (SLIPs) used for this analysis. Br is the Balearic Sea; Li is the Gulf of Lion; Lg is the Ligurian Sea; nTy is the northern Tyrrhenian Sea; sTy is the southern Thyrrenian Sea; Gb is the Gulf of Gabes; Io is the Ionian Sea; nAd is the northern Adriatic; sAd is the southern Adriatic Sea; Sr is Sardinia Island; Cr is Corsica Island; Si is Sicily Island.

period −10,000 to −8000 CE. From the model, it was possible to calculate the "central and western Mediterranean Sea-Level" (Med-SL), which represents the common signal found at all sites included in the model runs (Fig. 2a and Supplementary Table 2). The Med-SL, which is uniform over the entire central and western Mediterranean, absorbs a majority of the sea-level signal, whereas the regional signals (Fig. 2b, Supplementary Fig. 2) explain the variability we can observe at the basin scale. The model also estimates RSL for locations and times where there are no direct observations because it recognizes that an observation associated with a single point in space and time is informative about sea-level at proximal locations and times.

Med-SL estimates (Fig. 2a) indicate that the central and western Mediterranean sea-level rise decreased from $8.7 \pm 0.9\ \mathrm{mm\ a^{-1}}$ to $3.1 \pm 0.8\ \mathrm{mm\ a^{-1}}$ during the period −8000 to −5000 CE. The slowdown continued over subsequent millennia, with average rates of $1.5 \pm 0.8\ \mathrm{mm\ a^{-1}}$ between −5000 and −2000 CE, $0.5 \pm 0.7\ \mathrm{mm\ a^{-1}}$ between −2000 and 0 CE, and $0.45 \pm 0.7\ \mathrm{mm\ a^{-1}}$ in the last 2000 years. This stabilization trend reflects the general decrease in rates of global sea-level change consistent with the final phase of North American deglaciation and the consequent sudden reduction of meltwater input and with the stabilization of global mean surface temperature[7,21]. Between −2000 and 1850 CE, the ice-equivalent meltwater input is either zero or minimal[21,22]. During this period, Med-SL rise rates ranged between $0.30 \pm 0.7\ \mathrm{mm\ a^{-1}}$ and $0.55 \pm 0.6\ \mathrm{mm\ a^{-1}}$, while in the industrial-era (e.g., post 1850 CE) rates increased up to $1.05 \pm 0.6\ \mathrm{mm\ a^{-1}}$ (Fig. 2a, Supplementary Table 2). This acceleration closely mirrors post-industrial warming observed in several Mediterranean climatic proxies[12] and is consistent with the data extracted from the longest central and western Mediterranean tide-gauge data, which indicate sea-level rise rates of about 1.2–1.3 $\mathrm{mm\ a^{-1}}$[23,24] for the period 1880–2012 CE. Even higher rates (1.7–1.8 $\mathrm{mm\ a^{-1}}$) are observed for the second part of the last century, indicated by a larger dataset of tidal gauges and satellite altimetry[25,26]. This indicates that, at the basin scale, the mean estimate of industrial-era sea-level rising rate has no equivalent analog during the last 4000 years and that the rate of central and western Mediterranean industrial-era sea-level rise is unlikely (~25% probability) to be a random occurrence (Supplementary Fig. 3).

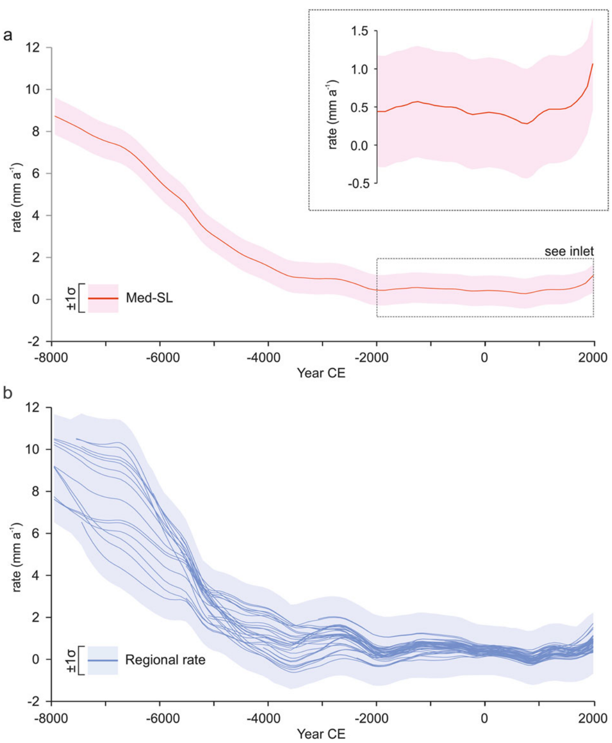

Fig. 2 Rates of relative sea-level change for the central and western Mediterranean region in the last 10,000 years. a Common sea-level signal (Med-SL). The inlet graph shows the Med-SL variation in the last 4000 years. The solid line and shaded envelope denote the model mean and the 1σ uncertainty (see Supplementary Table 2). **b** variability of relative sea-level (RSL) change rates in the 48 central and western Mediterranean regions included in the analysis. The solid line and shaded envelope are the model mean and 1 s uncertainty.

Our analysis highlights significant variability in the regional rates of sea-level change (Fig. 2b, Supplementary Fig. 2), which resulted in contrasting sea-level rising trends in the different portions of the Mediterranean basin analyzed in this study. Between −8000 and −5000 CE, faster sea-level rise rates were observed in the mid-western portion of the basin (<~10° E) with rates of $8.0 \pm 0.4\ \mathrm{mm\ a^{-1}}$ (Fig. 3). During the same period, sea-level rose much slower in the eastern portion of the basin (>~10° E) with rates that did not exceed $5.0 \pm 0.5\ \mathrm{mm\ a^{-1}}$ (Fig. 3). We then observed an inversion in this rising pattern after sea-level stabilized around −5000 CE. Since that period, rates of sea-level rise were always slower in the western portion of the basin (<~5° E) compared to the mid-eastern part (>~5°E, Fig. 3). These differences are particularly significant between −5000 and −2000 CE when low average rise rates ($0.5 \pm 0.2\ \mathrm{mm\ a^{-1}}$) are recorded in the Balearic Sea while high average rates ($2.0 \pm 0.3\ \mathrm{mm\ a^{-1}}$) characterize the Ionian Sea. In the last 4000 years, we observed a progressive decrease in the spatial variability of the rising with maximum average rates ($0.8 \pm 0.2\ \mathrm{mm\ a^{-1}}$) still recorded in the Ionian Sea, while minimal average rates ($0.2 \pm 0.2\ \mathrm{mm\ a^{-1}}$) are recorded both in the Balearic Sea and in the Gulf of Gabes (Fig. 3). We remark that the Gulf of Gabes, in Tunisia, represents a unique setting within the Mediterranean, as it is the only Mediterranean region where a purely isostatic mid-Holocene highstand is recorded, mediated by continental levering effects[27].

Sediment compaction and tectonics may have a role in controlling the observed spatial variability of sea-level change rates among regions. However, these components were minimized in our SLIPs database by prioritizing samples that are virtually incompressible or less prone to compaction, and by excluding data from regions that are significantly affected by co-seismic or volcano-tectonic vertical ground motions (see "Methods"). For this reason, much of the observed spatial variability of sea-level change rates is related to glacio- and hydro-isostatic adjustment (GIA), which has been the dominant process influencing the Mediterranean RSL evolution since the global mean sea-level stabilization of the mid-Holocene[7,23]. Our data indicate a general eastward increase of the GIA component in the central and western Mediterranean basin with minimal isostatic-driven subsidence recorded along the Spanish coast and in the Balearic Islands and maximum rates recorded in the Ionian Sea. This pattern differs from the one proposed by the available GIA models[7,28] which predict the maximal GIA-related sea-level change, with comparable magnitude, in the Ionian Sea and in the area comprising the Balearic, Sardinia and Corsica islands (Supplementary Fig. 3). The offset between the data and models is probably related to lateral variations in mantle viscosity and/or in the thickness of the lithosphere, which are currently not taken into account by Mediterranean GIA models[15,29]. Lateral heterogeneity of the Earth's mantle may significantly affect the Earth's response to deglaciation[30,31]. Our results can thus be employed for an improved tuning of geophysical predictions of RSL evolution in the basin, which is characterized by significant variability in lithospheric thickness and complex mantle

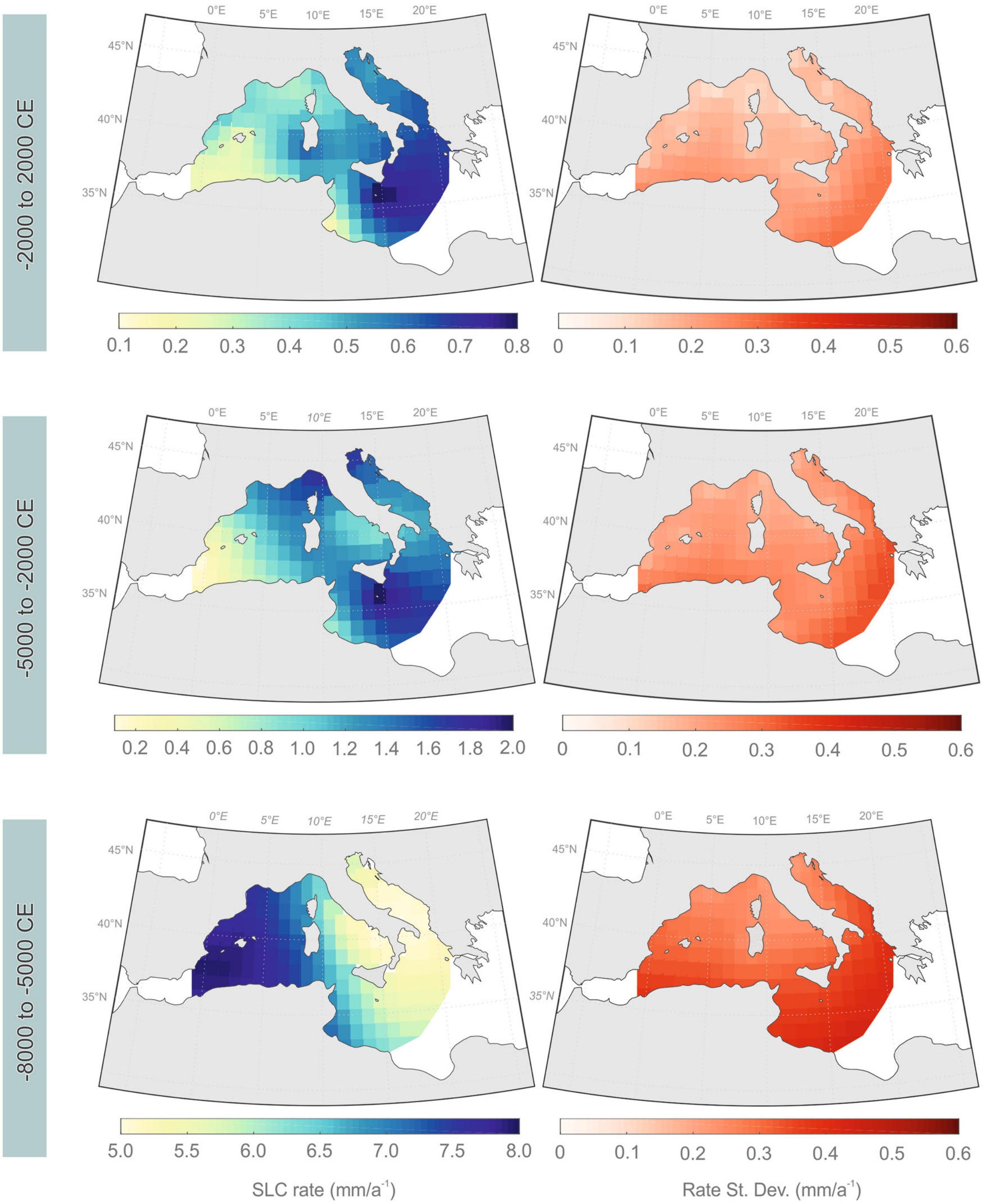

Fig. 3 Spatial and temporal variability of relative sea-level (RSL) changes and their uncertainties across the central and western Mediterranean basin in the time periods 2000 to −2000 CE, −2000 to −5000 CE, and −5000 to −8000 CE. Note the changes of scale for the different time intervals.

structure[19]. Nonetheless, it should be noted that our analysis has some geographic limitations due to the absence of SLIPs along much of the African coast and near the Gibraltar Strait.

Regional climatic influence on sea-level rise rates. Notwithstanding regional differences, our spatio-temporal analysis shows that the central and western Mediterranean regions were characterized by several sea-level oscillations in the last 6 millennia (Supplementary Fig. 2). Looking for the source of these sea-level oscillations, isostatic processes can be excluded. Isostasy is, by definition, a progressive and slow viscoelastic response of the Earth to the redistribution of ice and ocean loads[32,33]. GIA modeling is unable to resolve the scale of sea-level fluctuations observed, and the oscillatory patterns observed have a period that is too short to be influenced by glacio-isostatic processes. The fact that these fluctuations were observed across all regions would also exclude potential local tectonic influences and compaction-related subsidence. Instead, we suggest that regional climatic forcings are the most likely mechanism driving the variability in the sea-level change data.

In effect, while it is known that large ice melting was minimal after −2000 CE[21,34], much less is known about the responses to shorter-term Mediterranean climatic changes[35,36] such as the Roman Warm Period (RWP, ~−500 CE to ~500 CE), the Late Antique Little Ice Age (LALIA, ~536 to ~660 CE), the Medieval Climate Anomaly (MCA, ~860 to ~1250 CE) and the Little Ice

Age (LIA, ~1250 to ~1850 CE). In the Common Era, Med-SL rise rates varied within a range of ~0.9 mm a^{-1} (Supplementary Table 2, Fig. 4). Rise rates up to 0.5 ± 0.7 mm a^{-1} characterized the warmer episode occurring at the RWP while we observed a deceleration of the sea-level change rates (0.3 ± 0.7 mm a^{-1}) during the LALIA (Fig. 4). The LALIA is recognized as one of the most important cooling episodes of the Common Era[36]. This cooling event is found in different proxies (Fig. 4) such as temperature anomalies in Europe[37], and specifically in the central and western Mediterranean[38,39] and the European Alps[36]. During this period, we also observe a decrease in sea-surface temperatures (SSTs) in the western Mediterranean[40], as well as the exceptional seventh-century solar minimum[41].

The rising trend only returned to values similar to the pre-LALIA (0.45 ± 0.7 mm a^{-1}) during the MCA which was characterized by warmer climatic conditions (Fig. 4) and remained at similar values for much of the LIA (1250–1600 CE) suggesting a negligible influence of this cooling episode on central and western Mediterranean sea-level rise rates. In the remaining part of the pre-industrial period (1600 and 1800 CE) rates rose to 0.6 ± 0.6 mm a^{-1} while we observed a progressive acceleration of sea-level rise in the industrial-era, with rates up to 1.05 ± 0.6 mm a^{-1} (Fig. 4), which are significantly faster than any warm climatic episode of the Common Era.

Our spatio-temporal analysis shows a strong relationship between Mediterranean temperatures and the rate of sea-level rise

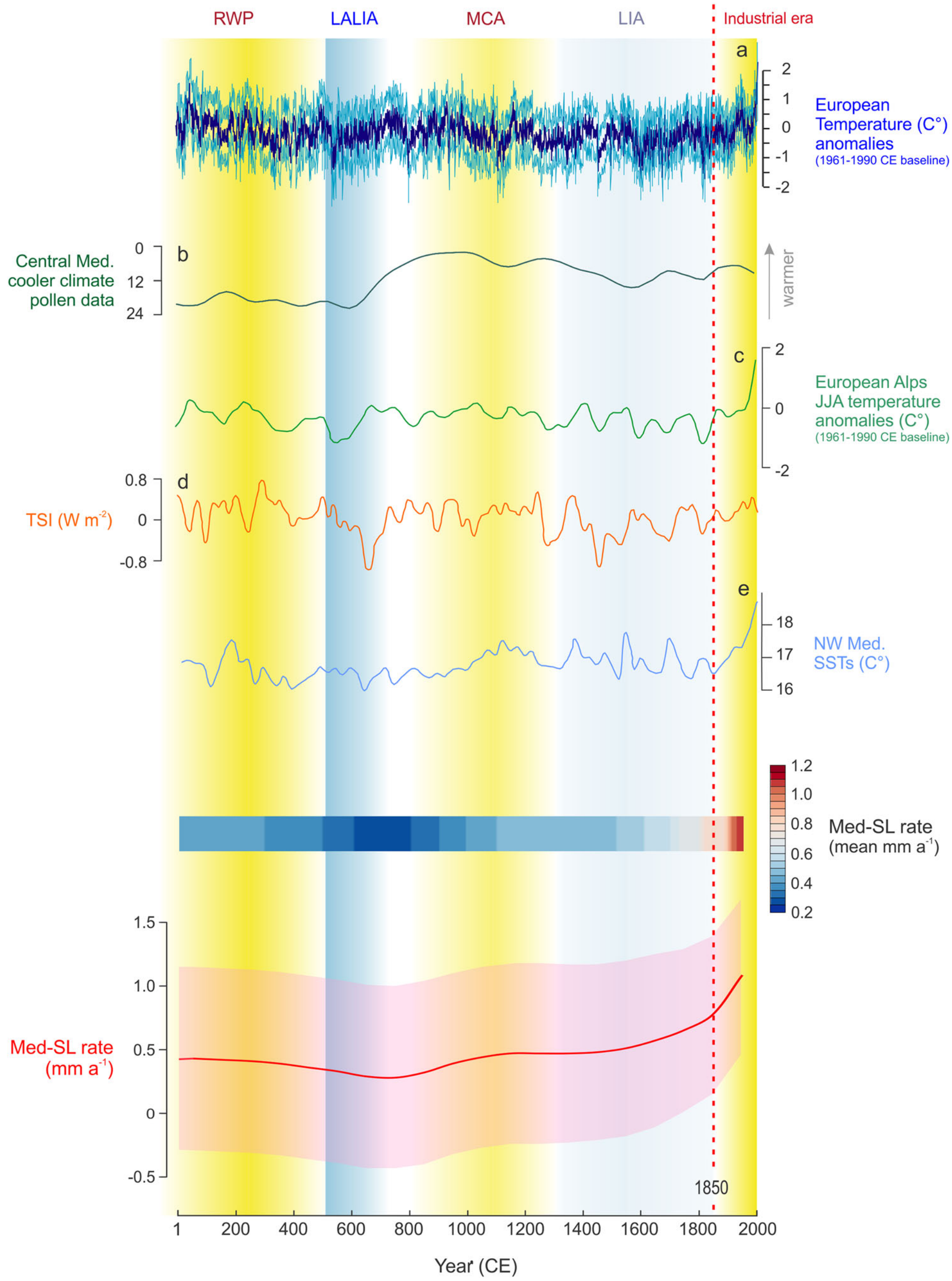

Fig. 4 Reconstructed variability of common sea-level signal (Med-SL) for the central and western Mediterranean region in the Common Era. Solid line and shaded envelope are the model mean and 1 s uncertainty. Med-SL is compared with **a** European Temperature anomalies[37], **b** central Mediterranean cooler climate pollen data[38], **c** summer (JJA) temperature anomalies in the European Alps[36], **d** total solar irradiance[41], **e** sea-surface temperatures (SSTs) in the western Mediterranean[40]. Temporal extension of the Roman Warm Period (RWP), the Late Antique Little Ice Age (LALIA), the Medieval Climate Anomaly (MCA), the Little Ice Age (LIA), and the Industrial period are from refs. [35,36]. The graded bar is the Med-SL model mean.

confirming, at the basin scale, the results locally obtained in the northwestern Adriatic Sea[42]. These oscillations are thus controlled by the differential response of Mediterranean sea-level to cooling/warming episodes, as demonstrated by the variability of sea-level rise rates observed in the Common Era.

Therefore, our findings suggest that a deeper exploration of the regional climatic parameters, controlling the variability of rise rates, is required to produce robust predictions of Mediterranean sea-level evolution in a changing climate. Regionally, global predictions of sea-level rise may be worsened by the expected increased warming of the Mediterranean[9]. This may have major implications for the near-future resilience of both natural and human-modified Mediterranean coasts, characterized by a narrow littoral area with high concentrations of people and assets and by rapid demographic, social, economic, and environmental change[43,44].

Methods

SLIPs database. We collated a database of SLIPs following the most recent standards in sea-level studies[18,45]. The analysis of a wide range of geological and archeological proxies[46–133] resulted in a database of 401 SLIPs (Supplementary Table 1) that identify the position of former RSL in the central and western Mediterranean coasts from 12 ka to present (Supplementary Fig. 1b). Mediterranean SLIPs are commonly derived from cores on coastal and alluvial plains, coastal marshes, and lagoons. For these samples, the definition of the indicative meaning is based on paleoecology and, in particular, on the macro-and micro-faunal assemblages (i.e., malacofauna, foraminifera, and ostracod assemblages). Furthermore, fossil intertidal bioconstructions (e.g., vermetids and *Lithophyllum byssoides* rims) and beachrocks have also yielded SLIPs for the Mediterranean region[15,16]. Finally, we produced SLIPs using maritime archeological structures whose functioning height is related to the former mean sea level such as fishtanks[20] or when found covered by fossil biological encrustations which clearly define the relationship with the former tidal frame[134]. We did not include samples from sectors manifesting major evidence for co-seismic land-level changes and/or crustal movements controlled by volcanic activity[135,136], which can generate significant departures from climatic-driven sea-level changes. Sediment compaction can be an important issue because it can lower the SLIP relative to the initial depositional elevation, resulting in an overestimation of the sea-level rise[18,137]. In the database compilation, we prioritized "base of basal" samples, e.g., those recovered from sedimentary units overlying incompressible substrates such as Pleistocene sands/gravels or rocky basements. These samples are, therefore, less prone to compaction[6]. Where basal samples were not available, we used intercalated samples which are derived from facies of low-density, organic-rich sediment within a sequence of higher density, clastic units[18,137], and are, therefore, susceptible to compaction. However, in the presence of two or more coeval intercalated SLIPs in the same region, we excluded those found at lower elevation as being affected by post-depositional compaction[137]. This procedure was of particular importance for the Rhone, Ebro, and Tiber deltas, for Venice lagoon, and for the Romagna and Versilia coastal plains. This practice allowed us to significantly reduce the effects of compaction on the SLIPs dataset. The fossil intertidal bioconstructions, beachrocks, and archeological structures are not subject to compaction. To perform a high-resolution assessment of variability in sea-level rise rates we clustered the data into 48 sub-regions, based on SLIPs collected no more than ~50 km apart (Supplementary Fig. 1a).

Spatio-temporal statistical model. We employed an empirical spatio-temporal hierarchical model[16] to reconstruct the common sea-level change across the central and western Mediterranean Basin, sub-regional variability in RSL changes, and spatial-temporal variability patterns in rates of RSL change across the basin over the last 10 ka. The height and timing (with vertical and temporal errors) of paleo-RSL from the 401 SLIPs from 48 sub-regions in the central and western Mediterranean database were fed into the model. Additional model inputs came from tide-gauge records taken from the Permanent Service for Mean Sea Level (PSMSL) (see Kopp et al.[3] for more details). Spatio-temporal variabilities of RSL change and their uncertainties (Fig. 3) are calculated through a linear transformation of the RSL predictions.

The hierarchical model has three levels: (i) a process level, which models RSL through space and time; (ii) a data level, which models how RSL from the process model is recorded by geological proxies; and (iii) a hyperparameter level, which describes the prior expectations for spatial and temporal RSL variability.

The process model represents the RSL field as the sum of three components, each with a Gaussian Process (GP) prior:

$$f(x,t) = g_b(t) + r_s(x,t) + r_f(x,t) \qquad (1)$$

where $\boldsymbol{x}$ represents a spatial location and $\boldsymbol{t}$ represents time. The three components that comprise the RSL field are g_b, which is the common Med-SL signal; $r_s(x, t)$, which represents the sub-regionally varying, slow, and temporally non-linear SL field; and $r_f(x, t)$, which represents the sub-regionally varying, fast and temporally non-linear SL field. As in Kopp et al.[3], the data model represents observations ($\boldsymbol{y_i}$) as:

$$y_i = f(x_i, t_i) + w(x_i, t_i) + y_0(x_i) + \varepsilon_i^y \qquad (2)$$

where x_i and t_i are the location and time, respectively, of observation i, $w(x, t)$ is a white noise term that captures sub-decadal changes in RSL and vertical errors beyond those nominally represented in the database, and $y_o(x_i)$ is a site-specific datum offset. ε_i^y represents errors in sea-level observations, and the term for time t_i is the sum of the mean observed age and an error term for time. As in Kopp et al.[3], geochronological uncertainties are incorporated using the noisy-input GP method[138], which translates errors in the independent variable into comparable errors in the dependent variable.

Hyperparameters that define prior knowledge of the amplitude and spatio-temporal scales for sea-level in each term of the process model were optimized via maximum likelihood. Optimized prior standard deviations for the common, slow, fast, and white noise terms were 10.4 m, 1.72 m, 2 cm, and 7 mm, respectively. The optimized temporal scales for the common, slow, and fast components were 12200, 3590, and 14.1 years, respectively, while the optimized spatial scales for the slow and fast components were 14° and 2° angular distances, respectively.

Data availability

Data related to this article can be found in Supplementary Table 1 (SLIP database) and Supplementary Table 2 (Med-SL rates). The references of the original papers used to produce the SLIP database are provided at the end of Supplementary Table 1. These data are available under a CC-BY 4.0 license at the following https://doi.org/10.5281/zenodo.4737120.

Code availability

The code used for analysis in this article is archived on GitHub (https://github.com/bobkopp/CESL-STEHM-GP).

Received: 18 January 2021; Accepted: 26 May 2021;
Published online: 29 June 2021

References

1. Church, J. A. & White, N. J. A 20th century acceleration in global sea-level rise. *Geophys. Res. Lett.* **33**, https://doi.org/10.1029/2005GL024826 (2006).
2. Kemp, A. C. et al. Climate related sea-level variations over the past two millennia. *Proc. Natl Acad. Sci. USA* **108**, 11017–11022 (2011).
3. Kopp, R. E. et al. Temperature-driven global sea-level variability in the Common Era. *Proc. Natl Acad. Sci. USA* **113**, E1434–E1441 (2016).
4. Kench, P. S. et al. Climate-forced sea-level lowstands in the Indian Ocean during the last two millennia. *Nat. Geosci.* **13**, 61–64 (2020).
5. Mitrovica, J. X. et al. On the robustness of predictions of sea level fingerprints. *Geophys. J. Int.* **187**, 729–742 (2011).
6. García-Artola, A. et al. Holocene sea-level database from the Atlantic coast of Europe. *Quat. Sci. Rev.* **196**, 177–192 (2018).
7. Roy, K. & Peltier, W. R. Relative sea level in the Western Mediterranean basin: a regional test of the ICE-7G_NA (VM7) model and a constraint on late Holocene Antarctic deglaciation. *Quat. Sci. Rev.* **183**, 76–87 (2018).
8. Horton, B. P. et al. Mapping sea-level change in time, space, and probability. *Annu. Rev. Environ. Resour.* **43**, 481–521 (2018).
9. Cramer, W. et al. Climate change and interconnected risks to sustainable development in the Mediterranean. *Nat. Clim. Change* **8**, 972–980 (2018).
10. Adloff, F. et al. Mediterranean Sea response to climate change in an ensemble of twenty first century scenarios. *Clim. Dyn.* **45**, 2775–2802 (2015).
11. Guiot, J. & Cramer, W. Climate change: the 2015 Paris Agreement thresholds and Mediterranean basin ecosystems. *Science* **354**, 465–468 (2016).
12. Lionello, P. & Scarascia, L. The relation between climate change in the Mediterranean region and global warming. *Regional Environ. Change* **18**, 1481–1493 (2018).
13. Anzidei, M. et al. Sea level rise scenario for 2100 AD in the heritage site of Pyrgi (Santa Severa, Italy). *J. Mar. Sci. Eng.* **8**, 64 (2020).
14. Eyring, V. et al. Overview of the Coupled Model Intercomparison Project Phase 6 (CMIP6) experimental design and organization. *Geoscientific Model Dev.* **9**, 1937–1958 (2016).
15. Vacchi, M. et al. New relative sea-level insights into the isostatic history of the Western Mediterranean. *Quat. Sci. Rev.* **201**, 396–408 (2018).
16. Vacchi, M. et al. Multiproxy assessment of Holocene relative sea-level changes in the western Mediterranean: sea-level variability and improvements in the definition of the isostatic signal. *Earth-Sci. Rev.* **155**, 172–197 (2016).
17. Ashe, E. L. et al. Statistical modeling of rates and trends in Holocene relative sea level. *Quat. Sci. Rev.* **204**, 58–77 (2019).

18. Shennan, I., Long, A. J. & Horton, B. P. *Handbook of Sea-level Research* Ch. 1 (John Wiley & Sons, 2015).
19. Faccenna, C. et al. Mantle dynamics in the Mediterranean. *Rev. Geophysics* **52**, 283–332 (2014).
20. Benjamin, J. et al. Late Quaternary sea-level changes and early human societies in the central and eastern Mediterranean Basin: an interdisciplinary review. *Quat. Int.* **449**, 29–57 (2017).
21. Peltier, W. R. Global glacial isostasy and the surface of the ice-age Earth: the ICE-5G (VM2) model and GRACE. *Annu. Rev. Earth Planet. Sci.* **32**, 111–149 (2004).
22. Milne, G. A., Long, A. J. & Bassett, S. E. Modelling Holocene relative sea-level observations from the Caribbean and South America. *Quat. Sci. Rev.* **24**, 1183–1202 (2005).
23. Marcos, M. & Tsimplis, M. N. Coastal sea level trends in Southern Europe. *Geophys. J. Int.* **175**, 70–82 (2008).
24. Zerbini, S. et al. Sea-level change in the Northern Mediterranean Sea from long-period tide gauge time series. *Earth-Sci. Rev.* **167**, 72–87 (2017).
25. Wöppelmann, G. & Marcos, M. Coastal sea level rise in southern Europe and the nonclimate contribution of vertical land motion. *J. Geophys. Res. Oceans* **117**, https://doi.org/10.1029/2011JC007469 (2012).
26. Anzidei, M. et al. Coastal structure, sea-level changes and vertical motion of the land in the Mediterranean. *Geolog. Soc. Lond., Spec. Publ.* **388**, 453–479 (2014).
27. Stocchi, P., Colleoni, F. & Spada, G. Bounds on the time–history and Holocene mass budget of Antarctica from sea-level records in SE Tunisia. *Pure Appl. Geophysics* **166**, 1319–1341 (2009).
28. Lambeck, K. & Purcell, A. Sea-level change in the Mediterranean Sea since the LGM: model predictions for tectonically stable areas. *Quat. Sci. Rev.* **24**, 1969–1988 (2005).
29. Stocchi, P. et al. MIS 5e relative sea-level changes in the Mediterranean Sea: contribution of isostatic disequilibrium. *Quat. Sci. Rev.* **185**, 122–134 (2018).
30. Spada, G., Antonioli, A., Cianetti, S. & Giunchi, C. Glacial isostatic adjustment and relative sea-level changes: the role of lithospheric and upper mantle heterogeneities in a 3-D spherical Earth. *Geophys. J. Int.* **165**, 692–702 (2006).
31. Kuchar, J., Milne, G. & Latychev, K. The importance of lateral Earth structure for North American glacial isostatic adjustment. *Earth Planet. Sci. Lett.* **512**, 236–245 (2019).
32. Milne, G. A. & Mitrovica, J. X. Postglacial sea-level change on a rotating Earth. *Geophys. J. Int.* **133**, 1–19 (1998).
33. Melini, D. & Spada, G. Some remarks on Glacial Isostatic Adjustment modelling uncertainties. *Geophys. J. Int.* **218**, 401–413 (2019).
34. Lambeck, K., Rouby, H., Purcell, A., Sun, Y. & Sambridge, M. Sea level and global ice volumes from the Last Glacial Maximum to the Holocene. *Proc. Natl Acad. Sci. USA* **111**, 15296–15303 (2014).
35. Margaritelli, G. et al. Marine response to climate changes during the last five millennia in the central Mediterranean Sea. *Glob. Planet. Change* **142**, 53–72 (2016).
36. Büntgen, U. et al. Cooling and societal change during the Late Antique Little Ice Age from 536 to around 660 AD. *Nat. Geosci.* **9**, 231–236 (2016).
37. Luterbacher, J. et al. European summer temperatures since Roman times. *Environ. Res. Lett.* **11**, 024001 (2016).
38. Kaniewski, D. et al. Solar pacing of storm surges, coastal flooding and agricultural losses in the Central Mediterranean. *Sci. Rep.* **6**, 25197 (2016).
39. Kaniewski, D. et al. Recent anthropogenic climate change exceeds the rate and magnitude of natural Holocene variability on the Balearic Islands. *Anthropocene* **32**, 100268 (2020).
40. Sicre, M. A. et al. Sea surface temperature variability in the North Western Mediterranean Sea (Gulf of Lion) during the Common Era. *Earth Planet. Sci. Lett.* **456**, 124–133 (2016).
41. Steinhilber, F., Beer, J. & Fröhlich, C. Total solar irradiance during the Holocene. *Geophysi. Res. Lett.* **36**, https://doi.org/10.1029/2009GL040142 (2009).
42. Faivre, S., Bakran-Petricioli, T., Barešić, J., Horvatić, D. & Macario, K. Relative sea-level change and climate change in the Northeastern Adriatic during the last 1.5 ka (Istria, Croatia). *Quat. Sci. Rev.* **222**, 105909 (2019).
43. Wolff, C. et al. A Mediterranean coastal database for assessing the impacts of sea-level rise and associated hazards. *Sci. Data* **5**, 180044 (2018).
44. Furlan, E. et al. Development of a Multi-Dimensional Coastal Vulnerability Index: assessing vulnerability to inundation scenarios in the Italian coast. *Sci. Total Environ.* **772**, 144650 (2021).
45. Khan, N. S. et al. Inception of a global atlas of sea levels since the Last Glacial Maximum. *Quat. Sci. Rev.* **220**, 359–371 (2019).
46. Ferrer-García, C. & Blázquez-Morilla, A. M. The evolution of the Albufereta lagoon (western Mediterranean): climate cycles and sea-level changes. *J. Coast. Res.* **28**, 1617–1626 (2012).
47. Brisset, E., Burjachs, F., Navarro, B. J. B. & de Pablo, J. F. L. Socio-ecological adaptation to Early-Holocene sea-level rise in the western Mediterranean. *Glob. Planet. change* **169**, 156–167 (2018).
48. Dupré, M., Fumanal, M. P., Sanjaume, E., Santisteban, C. & Usera, J. Quaternary evolution of Pego coastal lagoon (Southern Valencia, Spain). *Palaeogeogr. Palaeoclimatol. Palaeoecol.* **68**, 291–299 (1988).
49. Ruiz, J. M. & Carmona, P. La llanura deltaica de los ríos Júcar y Turia y la Albufera de Valencia. *Geomorfologia i Quat. litoral Homenatge al Dr. V. Rosselló* **1**, 399–419 (2005).
50. Marco-Barba, J., Holmes, J. A., Mesquita-Joanes, F. & Miracle, M. R. The influence of climate and sea-level change on the Holocene evolution of a Mediterranean coastal lagoon: evidence from ostracod palaeoecology and geochemistry. *Geobios* **46**, 409–421 (2013).
51. Sanjaume, E., Segura, F., Garcia, M. L. & Pardo, J. Recent sedimentation in Valencia Lagoon: preliminary results. *J. Coast. Res.* **8**, 688–698 (1992).
52. Carmona, P. & Ballester, J. P. Geomorphology, geoarchaeology and ancient settlement in the Valencian Gulf (Spain). *m.éditerranée. Rev. g.éographique des. pays m.éditerranéens./J. Mediterranean Geogr.* **117**, 61–72 (2011).
53. Rodríguez-Pérez, A., Blázquez, A. M., Guillem, J. & Usera, J. Maximum flood area during MIS 1 in the Almenara marshland (western Mediterranean): Benthic foraminifera and sedimentary record. *Holocene* **28**, 1452–1466 (2018).
54. Carmona, P. et al. Environmental evolution and mid–late Holocene climate events in the Valencia lagoon (Mediterranean coast of Spain). *Holocene* **26**, 1750–1765 (2016).
55. Blázquez, A. M., Rodríguez-Pérez, A., Torres, T. & Ortiz, J. E. Evidence for Holocene sea level and climate change from Almenara marsh (western Mediterranean). *Quat. Res.* **88**, 206–222 (2017).
56. Giaime, M. et al. In search of Pollentia's southern harbour: geoarchaeological evidence from the Bay of Alcúdia (Mallorca, Spain). *Palaeogeogr., Palaeoclimatol., Palaeoecol.* **466**, 184–201 (2017).
57. Yll, R., Pantaleón-Cano, J., Pérez-Obiol, R. P. & Roure, J. M. Cambio climático y transformación del medio durante el Holoceno en las Islas Baleares. Congrés del Neolític a la Península Ibérica. *Saguntum Extra* **2**, 45–51 (1999).
58. Burjachs, F., Pérez-Obiol, R., Roure, J. M. & Julià, R. Dinámica de la vegetación durante el Holoceno en la isla de Mallorca. *Trabajos de Palinología básica y aplicada* 199–210 (1994).
59. Cearreta, A., Benito, X., Ibáñez, C., Trobajo, R. & Giosan, L. Holocene palaeoenvironmental evolution of the Ebro Delta (Western Mediterranean Sea): evidence for an early construction based on the benthic foraminiferal record. *Holocene* **26**, 1438–1456 (2016).
60. Riera-Mora, S. & Esteban-Amat, A. Vegetation history and human activity during the last 6000 years on the central Catalan coast (northeastern Iberian Peninsula). *Vegetation Hist. Archaeobotany* **3**, 7–23 (1994).
61. Daura, J. et al. Palaeoenvironmental record of the Cal Maurici wetland sediment archive in Barcelona (NE Iberian Peninsula) between c. 6000 and 4000 cal. yr BP. *Holocene* **26**, 1020–1039 (2016).
62. Ejarque, A. et al. Coastal evolution in a Mediterranean microtidal zone: Mid to Late Holocene natural dynamics and human management of the Castelló lagoon, NE Spain. *PLoS ONE* **11**, e0155446 (2016).
63. Laborel, J. et al. Biological evidence of sea-level rise during the last 4500 years on the rocky coasts of continental southwestern France and Corsica. *Mar. Geol.* **120**, 203–223 (1994).
64. Sabatier, P. et al. Holocene evolution of a Languedocian lagoonal environment controlled by inherited coastal morphology (South of France). *Bull. de. la Soc. Geologique de. Fr.* **181**, 27–36 (2010).
65. Vella, C. & Provansal, M. Relative sea-level rise and neotectonic events during the last 6500 yr on the southern eastern Rhône delta, France. *Mar. Geol.* **170**, 27–39 (2000).
66. Amorosi, A., Rossi, V. & Vella, C. Stepwise post-glacial transgression in the Rhône Delta area as revealed by high-resolution core data. *Palaeogeogr., Palaeoclimatol., Palaeoecol.* **374**, 314–326 (2013).
67. Morhange, C., Laborel, J. & Hesnard, A. Changes of relative sea level during the past 5000 years in the ancient habour of Marseilles, Southern France. *Palaeogeogr., Palaeoclimatol., Palaeoecol.* **166**, 319–329 (2001).
68. Vella, C. et al. Evolution of the Rhône delta plain in the Holocene. *Mar. Geol.* **222**, 235–265 (2005).
69. Allinne et al. Archéologie et paléoenvironnement sur le site du pont romain des Esclapes (Fréjus, Var). *ArcheoSciences. Rev. d'archéom.étrie* **30**, 181–196 (2006).
70. Devillers, B., Excoffon, P., Morhange, C., Bonnet, S. & Bertoncello, F. Relative sea-level changes and coastal evolution at Forum Julii (Fréjus, Provence). *Comptes Rendus Geosci.* **339**, 329–336 (2007).
71. Morhange, C. et al. Relative sea-level changes during Roman times in the northwest Mediterranean: the 1st century AD fish tank of Forum Julii, Fréjus, France. *Geoarchaeology* **28**, 363–372 (2013).
72. Colombaroli, D., Marchetto, A. & Tinner, W. Long-term interactions between Mediterranean climate, vegetation and fire regime at Lago di Massaciuccoli (Tuscany, Italy). *J. Ecol.* **95**, 755–770 (2007).
73. Carboni, M. G. et al. Palaeoenvironmental reconstruction of late Quaternary foraminifera and molluscs from the ENEA borehole (Versilian plain, Tuscany, Italy). *Quat. Res.* **74**, 265–276 (2010).

74. Kaniewski, D. et al. Holocene evolution of Portus Pisanus, the lost harbour of Pisa. *Sci. Rep.* **8**, 11625 (2018).
75. Ghilardi, M. et al. Reconstructing the landscape evolution and the human occupation of the Lower Sagone River (Western Corsica, France) from the Bronze Age to the Medieval period. *J. Archaeological Sci.: Rep.* **12**, 741–754 (2017).
76. Ghilardi, M. et al. Enregistrements d'événements extrêmes et évolution des paysages dans les basses vallées fluviales du Taravo et du Sagone (Corse occidentale, France) au cours de l'âge du Bronze moyen à final: une perspective géoarchéologique. *Geomorphol. Relief, Process. Environ.* **23**, 15–35 (2017).
77. Vacchi, M., Ghilardi, M., Spada, G., Currás, A. & Robresco, S. New insights into the sea-level evolution in Corsica (NW Mediterranean) since the late Neolithic. *J. Archaeological Sci.: Rep.* **12**, 782–793 (2017).
78. Poher, Y., Ponel, P., Médail, F., Andrieu-Ponel, V. & Guiter, F. Holocene environmental history of a small Mediterranean island in response to sea-level changes, climate and human impact. *Palaeogeogr., Palaeoclimatol., Palaeoecol.* **465**, 247–263 (2017).
79. Lambeck, K., Anzidei, M., Antonioli, F., Benini, A. & Verrubbi, V. Tyrrhenian sea level at 2000 BP: evidence from Roman age fish tanks and their geological calibration. *Rendiconti Lincei. Sci. Fisiche e Nat.* **29**, 69–80 (2018).
80. Lambeck, K., Anzidei, M., Antonioli, F., Benini, A. & Esposito, A. Sea level in Roman time in the Central Mediterranean and implications for recent change. *Earth Planet. Sci. Lett.* **224**, 563–575 (2004).
81. Evelpidou, N. et al. Late Holocene sea level reconstructions based on observations of Roman fish tanks, Tyrrhenian Coast of Italy. *Geoarchaeology* **27**, 259–277 (2012).
82. Marra, F., Bozzano, F. & Cinti, F. R. Chronostratigraphic and lithologic features of the Tiber River sediments (Rome, Italy): implications on the post-glacial sea-level rise and Holocene climate. *Glob. Planet. Change* **107**, 157–176 (2013).
83. Salomon, F. Géoarchéologie du delta du Tibre: évolution géomorphologique holocène et contraintes hydrosédimentaires dans le système Ostie-Portus (Italie). Thèse de doctorat en géographie, option géoarchéologie. *Physio-Géo. Géographie Phys. et. Environ.* **8**, 1–6 (2014).
84. Goiran, J. P., Tronchère, H., Collalelli, U., Salomon, F. & Djerbi, H. Découverte d'un niveau marin biologique sur les quais de Portus: le port antique de Rome. *Méditerranée* **112**, 59–67 (2009).
85. De Muro, S. & Orrù, P. Il contributo delle Beach-Rock nello studio della risalita del mare olocenico. Le Beach-Rock post-glaciali della Sardegna nord-orientale. *Il Quaternario* **111**, 19–39 (1998).
86. Melis, R. T. et al. 8000 years of coastal changes on a western Mediterranean island: a multiproxy approach from the Posada plain of Sardinia. *Mar. Geol.* **403**, 93–108 (2018).
87. Melis, R. T., Depalmas, A., Di Rita, F., Montis, F. & Vacchi, M. Mid to late Holocene environmental changes along the coast of western Sardinia (Mediterranean Sea). *Glob. Planet. Change* **155**, 29–41 (2017).
88. Di Rita, F. & Melis, R. T. The cultural landscape near the ancient city of Tharros (central West Sardinia): vegetation changes and human impact. *J. Archaeological Sci.* **40**, 4271–4282 (2013).
89. De Falco, G. et al. Early cementation and accommodation space dictate the evolution of an overstepping barrier system during the Holocene. *Mar. Geol.* **369**, 52–66 (2015).
90. Ruiz, J. M., Carmona, P., Gómez-Bellard, C. & van Dommelen, P. Geomorfología y cambio ambiental en el entorno de los yacimientos púnicos de la llanura de Terralba (Golfo de Oristano, isla de Cerdeña, Italia). *Boletín Geol.ógico y. Min.* **129**, 331–352 (2018).
91. Orrù, P., Solinas, E., Puliga, G. & Deiana, G. Palaeo-shorelines of the historic period. Sant'Antioco Island, south-western Sardinia (Italy). *Quat. Int.* **232**, 71–81 (2011).
92. Orrù, P. E. et al. Sea level changes and geoarchaeology between the bay of Capo Malfatano and Piscinnì Bay (SW Sardinia) in the last 4 kys. *Quat. Int.* **336**, 180–189 (2014).
93. Orrù, P. E., Antonioli, F., Lambeck, K. & Verrubbi, V. Holocene sea-level change in the Cagliari coastal plain (southern Sardinia, Italy). *Quaternaria Nova* **8**, 193–212 (2004).
94. Barra, D. et al. The Versilian transgression in the Volturno river plain (Campania, Southern Italy): Palaeoenvironmental history and chronological data. *Il Quaternario* **9**, 445–458 (1996).
95. Sacchi, M. et al. Late-Holocene to recent evolution of Lake Patria, South Italy: an example of a coastal lagoon within a Mediterranean delta system. *Glob. Planet. Change* **117**, 9–27 (2014).
96. Barra, D. et al. Depositional history and palaeogeographic reconstruction of Sele coastal plain during Magna Grecia settlement of Hera Argiva (Southern Italy). *Geologica Romana* **35**, 151–166 (1999).
97. Amato, V. et al. Relative sea level changes and paleogeographical evolution of the southern Sele plain (Italy) during the Holocene. *Quat. Int.* **288**, 112–128 (2013).
98. Barra, D. et al. New data on the evolution of the Sele River coastal plain (southern Italy) during the Holocene. *Il Quaternario* **11**, 287–299 (1998).
99. Antonioli, F., Chemello, R., Improta, S. & Riggio, S. The Dendropoma (Mollusca Gastropoda, Vermetidae) intertidal reef formations and their paleoclimatological use. *Mar. Geol.* **161**, 155–170 (1999).
100. Basso, D., Bernasconi, M. P., Robba, E. & Marozzo, S. Environmental evolution of the Marsala sound, Sicily, during the last 6000 years. *J. Coast. Res.* **24**, 177–197 (2008).
101. Spampinato, C. R., Costa, B., Di Stefano, A., Monaco, C. & Scicchitano, G. The contribution of tectonics to relative sea-level change during the Holocene in coastal south-eastern Sicily: new data from boreholes. *Quat. Int.* **232**, 214–227 (2011).
102. Gerardi, F. et al. Geological record of tsunami inundations in Pantano Morghella (south-eastern Sicily) both from near and far-field sources. *Nat. Hazards Earth Syst. Sci.* **12**, 1185–1200 (2012).
103. Marriner, N., Gambin, T., Djamali, M., Morhange, C. & Spiteri, M. Geoarchaeology of the Burmarrad ria and early Holocene human impacts in western Malta. *Palaeogeogr., Palaeoclimatol., Palaeoecol.* **339**, 52–65 (2012).
104. Furlani, S. et al. Submerged speleothem in Malta indicates tectonic stability throughout the Holocene. *Holocene* **28**, 1588–1597 (2018).
105. Zaïbi, C. et al. Évolution du trait de côte à l'Holocène supérieur dans la Sebkha El-Guettiate de Skhira (Golfe de Gabès, Tunisie) à travers sa faune d'ostracodes et de foraminifères. *Geobios* **44**, 101–115 (2011).
106. Zaïbi, C. et al. Evolution of the sebkha Dreîaa (South-Eastern Tunisia, Gulf of Gabes) during the Late Holocene: response of ostracod assemblages. *Rev. de. micropaléontologie* **55**, 83–97 (2012).
107. Morhange, C. & Pirazzoli, P. A. Mid-Holocene emergence of southern Tunisian coasts. *Mar. Geol.* **220**, 205–213 (2005).
108. Strasser, A., Davaud, E. & Jedoui, Y. Carbonate cements in Holocene beachrock: example from Bahiret et Biban, southeastern Tunisia. *Sediment. Geol.* **62**, 89–100 (1989).
109. Lakhdar, R., Soussi, M., Ben Ismail, M. H. & M'Rabet, A. A Mediterranean Holocene restricted coastal lagoon under arid climate: case of the sedimentary record of Sabkha Boujmel (SE Tunisia). *Palaeogeogr., Palaeoclimatol., Palaeoecol.* **241**, 177–191 (2006).
110. Serandrei-Barbero, R., Albani, A., Donnici, S. & Rizzetto, F. Past and recent sedimentation rates in the Lagoon of Venice (Northern Italy). *Estuar., Coast. Shelf Sci.* **69**, 255–269 (2006).
111. McClennen, C. E. & Housley, R. A. Late-Holocene channel meander migration and mudflat accumulation rates, lagoon of Venice, Italy. *J. Coast. Res.* **224**, 930–945 (2006).
112. Zoppi, U. et al. Preliminary estimate of the reservoir age in the Lagoon of Venice. *Radiocarbon* **43**, 489–494 (2001).
113. Madricardo, F. & Donnici, S. Mapping past and recent landscape modifications in the Lagoon of Venice through geophysical surveys and historical maps. *Anthropocene* **6**, 86–96 (2014).
114. Tosi, L. Foglio geologico 128 Venezia e note illustrative. *Carta geologica d'Italia alla scala* **1**, 000 (2007).
115. Donnici, S., Serandrei-Barbero, R. & Canali, G. Evidence of climatic changes in the Venetian Coastal Plain (Northern Italy) during the last 40,000 years. *Sediment. Geol.* **281**, 139–150 (2012).
116. Galassi, P. & Marocco, R. Relative sea level rise and subsidence in the Caorle Lagoon (Northern Adriatic Sea), Italy, during Holocene. *Il Quaternario* **12**, 249–256 (1999).
117. Fontana, A. et al. Lagoonal settlements and relative sea level during Bronze age in Northern Adriatic: geoarchaeological evidence and paleogeographic constraints. *Quat. Int.* **439**, 17–36 (2017).
118. Fontana, A. & Zanferrari. A. *Foglio geologico 86 San Vito al Tagliamento e note illustrative*. *Carta geologica d'Italia alla scala 1:50,000* (2006).
119. Bondesan, A., Meneghel, M., Rosselli, R. & Vitturi. A. *Geomorphological Map of the Province of Venice, scale 1:50,000* (LAC, Firenze, 2004).
120. Furlani, S. et al. Tectonic effects on Late Holocene sea level changes in the Gulf of Trieste (NE Adriatic Sea, Italy). *Quat. Int.* **232**, 144–157 (2011).
121. Covelli, S., Fontolan, G., Faganeli, J. & Ogrinc, N. Anthropogenic markers in the Holocene stratigraphic sequence of the Gulf of Trieste (northern Adriatic Sea). *Mar. Geol.* **230**, 29–51 (2006).
122. Melis, R. et al. Sea level and paleoenvironment during roman times inferred from coastal archaeological sites in Trieste (northern Italy). *Alp. Mediterranean Quat.* **25**, 41–55 (2012).
123. Ogorelec, B., Faganeli, J., Mišič, M. & Čermelj, B. Reconstruction of paleoenvironment in the Bay of Koper (Gulf of Trieste, northern Adriatic). *Annales* **11**, e200 (1997).
124. Faivre, S. et al. Relative sea level change in western Istria (Croatia) during the last millennium. *Quat. Int.* **232**, 132–143 (2011).
125. Cibin, U. & Stefani, M. Foglio geologico 187 Codigoro e note illustrative. *Carta geologica d'Italia alla scala 1:50,000* (2009).
126. Correggiari, A., Roveri, M. & Trincardi, F. Late Pleistocene and Holocene evolution of the north Adriatic Sea. *Il Quaternario* **9**, 697–704 (1996).

127. Sarti, G., Centineo, M. C. & Calabrese, L. Foglio geologico 205 Comacchio e note illustrative. *Carta geologica d'Italia alla scala 1:50,000* (2009).
128. Marriner, N. et al. Post-Roman sea-level changes on Pag Island (Adriatic Sea): dating Croatia's "enigmatic" coastal notch? *Geomorphology* **221**, 83–94 (2014).
129. Faivre, S., Bakran-Petricioli, T., Horvatinčić, N. & Sironić, A. Distinct phases of relative sea level changes in the central Adriatic during the last 1500 years—influence of climatic variations? *Palaeogeogr. Palaeoclimatol. Palaeoecol.* **369**, 163–174 (2013).
130. Caldara, M., Caroli, I. & Simone, O. Holocene evolution and sea-level changes in the Battaglia basin area (eastern Gargano coast, Apulia, Italy). *Quat. Int.* **183**, 102–114 (2008).
131. Caldara, M. & Simone, O. Coastal changes in the eastern Tavoliere Plain (Apulia, Italy) during the Late Holocene: natural or anthropic? *Quat. Sci. Rev.* **24**, 2137–2145 (2005).
132. Di Rita, F., Simone, O., Caldara, M., Gehrels, W. R. & Magri, D. Holocene environmental changes in the coastal Tavoliere Plain (Apulia, southern Italy): a multiproxy approach. *Palaeogeogr., Palaeoclimatol., Palaeoecol.* **310**, 139–151 (2011).
133. Primavera, M., Simone, O., Fiorentino, G. & Caldara, M. The palaeoenvironmental study of the Alimini Piccolo lake enables a reconstruction of Holocene sea-level changes in southeast Italy. *Holocene* **21**, 553–563 (2011).
134. Morhange, C. & Marriner, N. *Handbook of Sea-level Research* Ch. 9 (John Wiley and Sons, 2015).
135. Scicchitano, G. et al. Uplifted Holocene shorelines at Capo Milazzo (NE Sicily, Italy): evidence of co-seismic and steady-state deformation. *Quat. Int.* **232**, 201–213 (2011).
136. Aucelli, P. P., Cinque, A., Mattei, G. & Pappone, G. Late Holocene landscape evolution of the gulf of Naples (Italy) inferred from geoarchaeological data. *J. Maps* **13**, 300–310 (2017).
137. Shennan, I. & Horton, B. Holocene land-and sea-level changes in Great Britain. *J. Quat. Sci.* **17**, 511–526 (2002).
138. McHutchon, A. & Rasmussen, C. Gaussian process training with input noise. *Adv. Neural Inf. Process. Syst.* **24**, 1341–1349 (2011).

Acknowledgements

M.V. is funded by the Rita Levi Montalcini program of the Italian Ministry of University and Research (MUR). A.R. thanks the Deutsche Forschungsgemeinschaft (Excellence Cluster "EXC 2077: The Ocean Floor—Earth's Uncharted Interface", project no. 390741603) for support. R.E.K. and K.J. were supported by US National Science Foundation grants DGE-1633557 and OCE-1804999. We further acknowledge PALSEA, a working group of the International Union for Quaternary Sciences (INQUA) and Past Global Changes (PAGES), which in turn received support from the Swiss Academy of Sciences and the Chinese Academy of Sciences.

Author contributions

M.V., K.J., R.E.K., and A.R. designed the research approach. M.V. led the research and wrote the first draft of the paper. M.V., N.M., D.K., and A.R. contributed to compiling the sea-level database. K.J. and R.E.K. performed the statistical analysis. M.V., K.J., R.E. K., N.M., D.K., and A.R. contributed to the writing of the manuscript.

Competing interests

The authors declare no competing interests.

Additional information

Supplementary information The online version contains supplementary material available at https://doi.org/10.1038/s41467-021-24250-1.

Correspondence and requests for materials should be addressed to M.V.

Peer review information *Nature Communications* thanks Marco Anzidei and the other, anonymous, reviewer(s) for their contribution to the peer review of this work.

Reprints and permission information is available at http://www.nature.com/reprints

Publisher's note Springer Nature remains neutral with regard to jurisdictional claims in published maps and institutional affiliations.

Vacchi's data base (401 points)

Nb	Sample	^{14}C age BP	± error (y)	Cal BC/AD	Error 1σ (yr)	Cal -2σ	Cal +2σ	ΔR	RSL (m)	± error (m)	1σ m (+)	1σ m (-)	Lat. N	Long. E	Location	Material	$\delta^{13}C$	Reg.	Reference	??
1	Beta-213544	N/A	N/A	-850	53	-956	-744	N/A	-1.40	1.00	1	1	38.36	-0.44	Pego-Albufereta	Peat	N/A	1	6	*
2	Beta-213540	N/A	N/A	757	103	551	963	N/A	-0.30	0.45	0.3	0.6	38.36	-0.44	Pego-Albufereta	Peat	N/A	1	6	*
3	Beta-46429	N/A	N/A	-5401	71	-5543	-5259	N/A	-3.00	1.10	1.1	1.1	38.87	0.08	Pego-Albufereta	Organics	N/A	1	7	
4	Poz-93699	N/A	N/A	-6202	141	-6484	-5920	N/A	-10.00	1.10	1.1	1.1	38.86	0.05	Pego-Albufereta	Organics	N/A	1	7	
5	Poz-93698	N/A	N/A	-6836	192	-7220	-6452	N/A	-16.60	1.10	1.1	1.1	38.82	0.03	Pego-Albufereta	Organics	N/A	1	7	
6	Poz-93965	N/A	N/A	-6842	187	-7216	-6468	N/A	-17.00	1.10	1.1	1.1	38.82	0.03	Pego-Albufereta	Organics	N/A	1	7	
7	Poz-93966	N/A	N/A	-6838	190	-7218	-6458	N/A	-17.50	1.10	1.1	1.1	38.82	0.03	Pego-Albufereta	Organics	N/A	1	7	
8	UBAR-44	N/A	N/A	-6737	291	-7319	-6155	N/A	-10.60	0.60	0.6	0.6	38.87	-0.06	Valencia Plain	Peat	N/A	2	8	*
9	UBAR-78	N/A	N/A	-7192	417	-8026	-6358	N/A	-16.10	0.60	0.6	0.6	38.87	-0.06	Valencia Plain	Peat	N/A	2	8	*
10	Beta-147301	N/A	N/A	-2885	351	-3587	-2183	N/A	-1.80	1.10	1.1	1.1	39.15	-0.25	Valencia Plain	Shell	N/A	2	9	*
11	Beta-215488	N/A	N/A	-1513	95	-1703	-1323	N/A	-0.90	0.60	0.6	0.6	39.3	-0.32	Valencia Plain	Pollen	N/A	2	10	*
12	Beta-208373	N/A	N/A	-5192	122	-5436	-4948	N/A	-3.50	0.50	0.5	0.5	39.3	-0.32	Valencia Plain	Pollen	N/A	2	10	*
13	Beta204241	N/A	N/A	-5550	69	-5688	-5412	N/A	-4.50	0.70	0.7	0.7	39.3	-0.32	Valencia Plain	Pollen	N/A	2	10	*
14	N/A	N/A	N/A	1318	349	620	2016	N/A	-1.30	1.00	1	1	39.34	-0.36	Valencia Plain	Shell	N/A	2	11	*
15	R-2176	N/A	N/A	-6388	295	-6978	-5798	N/A	-6.10	0.70	0.7	0.7	39.45	-0.33	Valencia Plain	Peat	N/A	2	12	*
16	R-2168	N/A	N/A	-2564	266	-3096	-2032	N/A	-2.10	0.70	0.7	0.7	39.45	-0.33	Valencia Plain	Peat	N/A	2	9	*
17	Beta-386336	N/A	N/A	-83	86	-255	89	N/A	-1.10	0.20	0.2	0.2	39.75	-0.18	Valencia Plain	Organics	N/A	2	13	**
18	Beta-346465	N/A	N/A	1132	90	952	1312	N/A	-0.50	0.50	0.5	0.5	39.39	-0.37	Valencia Plain	Plants	N/A	2	14	**
19	Beta-377886	N/A	N/A	592	53	486	698	N/A	-1.00	0.50	0.5	0.5	39.39	-0.37	Valencia Plain	Seeds	N/A	2	14	**
20	Beta-346466	N/A	N/A	-444	218	-880	-8	N/A	-1.50	0.50	0.5	0.5	39.39	-0.37	Valencia Plain	Shell	N/A	2	14	**
21	Beta-346467	N/A	N/A	-1826	180	-2186	-1466	N/A	-2.50	0.50	0.5	0.5	39.39	-0.37	Valencia Plain	Shell	N/A	2	14	**
22	Beta-362537	N/A	N/A	-2509	214	-2937	-2081	N/A	-2.70	1.00	1	1	39.39	-0.37	Valencia Plain	Shell	N/A	2	14	**
23	Beta-346464	N/A	N/A	-2702	174	-3050	-2354	N/A	-2.80	1.00	1	1	39.39	-0.37	Valencia Plain	Shell	N/A	2	14	**
24	Beta-346468	N/A	N/A	-6239	140	-6519	-5959	N/A	-4.60	0.70	0.7	0.7	39.39	-0.37	Valencia Plain	Organics	N/A	2	14	**
25	Beta-288410	N/A	N/A	-2889	127	-3143	-2635	N/A	-0.90	0.30	0.3	0.3	39.75	-0.18	Almenara	Organics	N/A	3	14	**
26	Beta-288412	N/A	N/A	-5552	65	-5682	-5422	N/A	-2.70	0.30	0.3	0.3	39.75	-0.18	Almenara	Organics	N/A	3	15	**
27	Poz-72248	N/A	N/A	969	162	645	1293	N/A	-0.20	0.60	0.2	1	39.83	3.11	Baleares	Shell	N/A	4	16	**
28	Poz-69098	N/A	N/A	624	145	334	914	N/A	-0.20	0.40	0.2	0.6	39.83	3.11	Baleares	Shell	N/A	4	16	**
29	Poz-69459	N/A	N/A	369	174	21	717	N/A	-0.80	0.60	0.6	0.6	39.83	3.11	Baleares	Shell	N/A	4	16	**
30	Poz-72246b	N/A	N/A	-26	166	-358	306	N/A	-0.40	0.80	0.4	1.2	39.83	3.11	Baleares	Shell	N/A	4	16	**
31	Beta-69334	N/A	N/A	-582	178	-938	-226	N/A	-2.00	1.20	1.2	1.2	39.83	3.11	Baleares	Organics	N/A	4	16	**
32	Poz-69099	N/A	N/A	-1205	188	-1581	-829	N/A	-0.50	0.75	0.5	1	39.83	3.11	Baleares	Shell	N/A	4	16	**
33	Poz-69465	N/A	N/A	-1302	179	-1660	-944	N/A	-0.50	0.75	0.5	1	39.83	3.11	Baleares	Shell	N/A	4	16	**
34	Poz-69460	N/A	N/A	-1468	52	-1572	-1364	N/A	-0.60	0.80	0.6	1	39.83	3.11	Baleares	Plant remains	N/A	4	16	**
35	Poz-69461	N/A	N/A	-1597	138	-1873	-1321	N/A	-0.80	0.90	0.8	1	39.83	3.11	Baleares	Plant remains	N/A	4	16	**
36	Poz-69454	N/A	N/A	-1790	98	-1986	-1594	N/A	-0.90	0.95	0.9	1	39.83	3.11	Baleares	Plant remains	N/A	4	16	**
37	Poz-69453	N/A	N/A	-1832	84	-2000	-1664	N/A	-0.60	0.80	0.6	1	39.83	3.11	Baleares	Plant remains	N/A	4	16	**
38	Poz-69541	N/A	N/A	-1958	70	-2098	-1818	N/A	-0.40	0.70	0.4	1	39.83	3.11	Baleares	Plant remains	N/A	4	16	**
39	Poz-69455	N/A	N/A	-2066	121	-2308	-1824	N/A	-1.10	1.00	1	1	39.83	3.11	Baleares	Plant remains	N/A	4	16	**
40	Poz-69470	N/A	N/A	-2504	220	-2944	-2064	N/A	-0.80	0.60	0.6	0.6	39.83	3.11	Baleares	Shell	N/A	4	16	**
41	Poz-69466	N/A	N/A	-2950	213	-3376	-2524	N/A	-1.10	1.00	1	1	39.83	3.11	Baleares	Shell	N/A	4	16	**
42	Poz-69472	N/A	N/A	-3301	192	-3685	-2917	N/A	-1.20	0.60	0.6	0.6	39.83	3.11	Baleares	Charcoal	N/A	4	16	**
43	Poz-72246	N/A	N/A	-3776	146	-4068	-3484	N/A	-1.20	1.00	1	1	39.83	3.11	Baleares	Shell	N/A	4	16	**
44	Poz-69473	N/A	N/A	-3899	121	-4141	-3657	N/A	-1.20	1.00	1	1	39.83	3.11	Baleares	Charcoal	N/A	4	16	**
45	Poz-69467b	N/A	N/A	-3947	267	-4481	-3413	N/A	-1.60	1.00	1	1	39.83	3.11	Baleares	Shell	N/A	4	16	**
46	Poz-69467	N/A	N/A	-4012	184	-4380	-3644	N/A	-1.50	1.00	1	1	39.83	3.11	Baleares	Shell	N/A	4	16	**
47	Ua-2729	N/A	N/A	-5146	310	-5766	-4526	N/A	-5.40	1.20	1.2	1.2	39.93	3.95	Baleares	Shell	N/A	4	17	**
48	ETH-11904	N/A	N/A	-5248	213	-5674	-4822	N/A	-3.60	1.20	1.2	1.2	39.83	3.11	Baleares	Organics	N/A	4	18	**
49	Ua-2732	N/A	N/A	-5962	242	-6446	-5478	N/A	-7.00	1.20	1.2	1.2	39.83	3.11	Baleares	Organics	N/A	4	18	**
50	Beta-380019	N/A	N/A	469	69	331	607	N/A	-0.10	0.35	0.1	0.6	40.7	0.6	Ebro delta	Shell	N/A	5	19	**
51	Beta-380020	N/A	N/A	441	95	251	631	N/A	-0.40	0.50	0.4	0.6	40.7	0.6	Ebro delta	Shell	N/A	5	19	**
52	Beta-348514	N/A	N/A	330	77	176	484	N/A	-0.50	0.55	0.5	0.6	40.7	0.6	Ebro delta	Shell	N/A	5	19	**
53	Beta-348515	N/A	N/A	242	103	36	448	N/A	-0.60	0.60	0.6	0.6	40.7	0.6	Ebro delta	Shell	N/A	5	19	**
54	Beta-380021	N/A	N/A	-672	126	-924	-420	N/A	-0.80	0.60	0.6	0.6	40.7	0.6	Ebro delta	Shell	N/A	5	19	**
55	Beta-348516	N/A	N/A	-645	136	-917	-373	N/A	-0.90	0.60	0.6	0.6	40.7	0.6	Ebro delta	Shell	N/A	5	19	**
56	GD-5918	N/A	N/A	1101	104	893	1309	N/A	-0.50	0.60	0.5	0.7	41.2	1.66	Cubelles	Organics	N/A	6	20	**
57	GD-6597	N/A	N/A	-498	305	-1108	112	N/A	-0.10	0.65	0.1	1.2	41.2	1.66	Cubelles	Organics	N/A	6	20	**
58	GD-7041	N/A	N/A	-2025	244	-2513	-1537	N/A	-1.20	1.20	1.2	1.2	41.2	1.66	Cubelles	Organics	N/A	6	20	**

59	GD-5919	N/A	N/A	-3818	151	-4120	-3516	N/A	-3.40	0.80	0.8	0.8	41.2	1.66	Cubelles	Organics	N/A	6	20	**
60	Poz-19098	N/A	N/A	-2943	68	-3079	-2807	N/A	-3.00	0.50	0.5	0.5	41.33	2.05	Barcelona	Organics	N/A	7	21	**
61	Poz-19180	N/A	N/A	-4022	199	-4420	-3624	N/A	-2.70	0.50	0.5	0.5	41.33	2.05	Barcelona	Organics	N/A	7	21	**
62	Poz-19247	N/A	N/A	-2991	98	-3187	-2795	N/A	-3.40	0.50	0.5	0.5	41.33	2.05	Barcelona	Organics	N/A	7	21	**
63	Beta-272094	N/A	N/A	1212	108	996	1428	N/A	-0.60	0.50	0.5	0.5	42.28	3.1	Empuries	Shell	N/A	8	22	**
64	Beta-272095	N/A	N/A	905	122	661	1149	N/A	-0.80	0.90	0.8	1	42.28	3.1	Empuries	Shell	N/A	8	22	**
65	Beta-286856	N/A	N/A	45	144	-243	333	N/A	-1.30	1.00	1	1	42.28	3.1	Empuries	Shell	N/A	8	22	**
66	Beta-272096	N/A	N/A	-603	161	-925	-281	N/A	-1.40	1.00	1	1	42.28	3.1	Empuries	Shell	N/A	8	22	**
67	Beta-286857	N/A	N/A	-2687	184	-3055	-2319	N/A	-2.60	0.50	0.5	0.5	42.28	3.1	Empuries	Plant remains	N/A	8	22	**
68	Beta-272097	N/A	N/A	-2852	156	-3164	-2540	N/A	-3.20	0.50	0.5	0.5	42.28	3.1	Empuries	Plant remains	N/A	8	22	**
69	LGQ-775	N/A	N/A	-327	161	-649	-5	N/A	-0.40	0.30	0.3	0.3	42.04	3.22	Empuries	L. byssoides	N/A	8	23	*
70	N/A	N/A	N/A	1489	130	1229	1749	N/A	0.00	0.30	0	0.6	43.5	3.86	Palavas-Languedoc	Shell	N/A	9	24	*
71	N/A	N/A	N/A	1308	105	1098	1518	N/A	-0.30	0.45	0.3	0.6	43.5	3.86	Palavas-Languedoc	Shell	N/A	9	24	*
72	N/A	N/A	N/A	652	125	402	902	N/A	-0.40	0.70	0.4	1	43.52	3.88	Palavas-Languedoc	Shell	N/A	9	24	*
73	N/A	N/A	N/A	409	151	107	711	N/A	0.00	0.50	0	1	43.52	3.88	Palavas-Languedoc	Shell	N/A	9	24	*
74	N/A	N/A	N/A	-835	130	-1095	-575	N/A	-0.60	0.80	0.6	1	43.52	3.88	Palavas-Languedoc	Shell	N/A	9	24	*
75	N/A	N/A	N/A	-1083	168	-1419	-747	N/A	-1.30	1.00	1	1	43.52	3.88	Palavas-Languedoc	Shell	N/A	9	24	*
76	N/A	N/A	N/A	-1471	151	-1773	-1169	N/A	-1.80	1.00	1	1	43.52	3.88	Palavas-Languedoc	Shell	N/A	9	24	*
77	N/A	N/A	N/A	-3892	141	-4174	-3610	N/A	-2.40	1.00	1	1	43.52	3.88	Palavas-Languedoc	Shell	N/A	9	24	*
78	N/A	N/A	N/A	-5526	102	-5730	-5322	N/A	-6.40	1.00	1	1	43.5	3.86	Palavas-Languedoc	Shell	N/A	9	24	*
79	LY-8447	N/A	N/A	810	140	530	1090	N/A	-0.10	0.30	0.1	0.5	43.45	4.89	RhoneDelta	Peat	N/A	10	25	*
80	LY-8731	N/A	N/A	-3304	201	-3706	-2902	N/A	-2.80	0.50	0.5	0.5	43.45	4.89	RhoneDelta	Peat	N/A	10	25	*
81	LY-8621	N/A	N/A	-3508	132	-3772	-3244	N/A	-3.10	0.50	0.5	0.5	43.45	4.89	RhoneDelta	Peat	N/A	10	25	*
82	LY-7081	N/A	N/A	-3967	255	-4477	-3457	N/A	-3.80	0.50	0.5	0.5	43.45	4.89	RhoneDelta	Peat	N/A	10	25	*
83	LY-8446	N/A	N/A	-4259	189	-4637	-3881	N/A	-4.70	0.50	0.5	0.5	43.45	4.89	RhoneDelta	Peat	N/A	10	25	*
84	LY-364	N/A	N/A	-4421	362	-5145	-3697	N/A	-5.10	0.50	0.5	0.5	43.45	4.89	RhoneDelta	Peat	N/A	10	25	*
85	LY-8218	N/A	N/A	-4863	135	-5133	-4593	N/A	-5.50	0.50	0.5	0.5	43.45	4.89	RhoneDelta	Peat	N/A	10	25	*
86	LY-8671	N/A	N/A	-5266	191	-5648	-4884	N/A	-6.40	0.50	0.5	0.5	43.45	4.89	RhoneDelta	Peat	N/A	10	25	*
87	LY-8681	N/A	N/A	-5546	70	-5686	-5406	N/A	-7.40	0.40	0.4	0.4	43.49	4.52	RhoneDelta	Peat	N/A	10	25	*
88	N/A	N/A	N/A	-8415	127	-8669	-8161	N/A	-33.80	1.20	1.2	1.2	43.45	4.38	RhoneDelta	Organics	N/A	10	26	*
89	N/A	N/A	N/A	-8455	147	-8749	-8161	N/A	-31.70	0.70	0.7	0.7	43.52	4.33	RhoneDelta	Organics	N/A	10	26	*
90	MC-2017	N/A	N/A	-8671	439	-9549	-7793	N/A	-29.90	0.40	0.4	0.4	43.49	4.52	RhoneDelta	Peat	N/A	10	28	*
91	POZ-3937	N/A	N/A	-8984	200	-9384	-8584	N/A	-39.50	0.40	0.4	0.4	43.49	4.52	RhoneDelta	Peat	N/A	10	28	*
92	N/A	N/A	N/A	-9084	207	-9498	-8670	N/A	-41.40	1.50	1.5	1.5	43.45	4.38	RhoneDelta	Organics	N/A	10	26	*
93	POZ-3938	N/A	N/A	-9226	81	-9388	-9064	N/A	-42.10	0.40	0.4	0.4	43.49	4.52	RhoneDelta	Peat	N/A	10	28	*
94	N/A	N/A	N/A	-9757	301	-10359	-9155	N/A	-43.30	1.50	1.5	1.5	43.45	4.38	RhoneDelta	wood	N/A	10	26	*
95	LGQ 906	N/A	N/A	1639	195	1249	2029	N/A	-0.20	0.25	0.2	0.3	43.29	5.37	Marseille	Shell	N/A	11	27	*
96	MC-697 A	N/A	N/A	87	302	-517	691	N/A	-0.40	0.30	0.3	0.3	43.29	5.37	Marseille	Shell	N/A	11	27	*
97	MC-697 B	N/A	N/A	-36	299	-634	562	N/A	-0.40	0.30	0.3	0.3	43.29	5.37	Marseille	Shell	N/A	11	27	*
98	N/A	N/A	N/A	500	50	400	600	N/A	-0.40	0.30	0.3	0.3	43.29	5.37	Marseille	ell on Roman q	N/A	11	27	*
99	N/A	N/A	N/A	-475	25	-525	-425	N/A	-0.70	0.30	0.3	0.3	43.29	5.37	Marseille	ell on Archaic q	N/A	11	27	*
100	N/A	N/A	N/A	-475	25	-525	-425	N/A	-0.80	0.30	0.3	0.3	43.29	5.37	Marseille	ll on wooden p	N/A	11	27	*
101	LY-9008	N/A	N/A	-831	265	-1361	-301	N/A	-0.80	0.30	0.3	0.3	43.29	5.37	Marseille	Shell	N/A	11	27	*
102	LY-8374	N/A	N/A	-1742	258	-2258	-1226	N/A	-1.50	0.30	0.3	0.3	43.29	5.37	Marseille	Mesophyllum	N/A	11	27	*
103	LY-8423	N/A	N/A	-2676	247	-3170	-2182	N/A	-1.70	0.30	0.3	0.3	43.29	5.37	Marseille	Shell	N/A	11	27	*
104	N/A	N/A	N/A	1660	50	1560	1760	N/A	-0.20	0.30	0.3	0.3	43.29	5.37	Marseille	Shell on ditch	N/A	11	27	*
105	LGQ-802	N/A	N/A	1332	78	1176	1488	N/A	-0.20	0.30	0.2	0.4	43.16	5.58	La Ciotat-Hyères	L. byssoides	N/A	12	23	*
106	LGQ-801	N/A	N/A	1098	114	870	1326	N/A	-0.30	0.35	0.3	0.4	43.16	5.58	La Ciotat-Hyères	L. byssoides	N/A	12	23	*
107	LGQ-799	N/A	N/A	1391	94	1203	1579	N/A	-0.30	0.35	0.3	0.4	43.16	5.58	La Ciotat-Hyères	L. byssoides	N/A	12	23	*
108	LGQ-800	N/A	N/A	669	105	459	879	N/A	-0.40	0.40	0.4	0.4	43.16	5.58	La Ciotat-Hyères	L. byssoides	N/A	12	23	*
109	LGQ-797	N/A	N/A	1372	75	1222	1522	N/A	-0.40	0.40	0.4	0.4	43.16	5.58	La Ciotat-Hyères	L. byssoides	N/A	12	23	*
110	LGQ-798	N/A	N/A	826	143	540	1112	N/A	-0.40	0.40	0.4	0.4	43.16	5.58	La Ciotat-Hyères	L. byssoides	N/A	12	23	*
111	LGQ-760	N/A	N/A	-1695	197	-2089	-1301	N/A	-1.10	0.40	0.4	0.4	43.16	5.58	La Ciotat-Hyères	L. byssoides	N/A	12	23	*
112	LGQ-763	N/A	N/A	-1713	179	-2071	-1355	N/A	-1.30	0.40	0.4	0.4	43.16	5.58	La Ciotat-Hyères	L. byssoides	N/A	12	23	*
113	LGQ-761	N/A	N/A	-1463	162	-1787	-1139	N/A	-1.30	0.40	0.4	0.4	43.16	5.58	La Ciotat-Hyères	L. byssoides	N/A	12	23	*
114	LGQ-773	N/A	N/A	1167	122	923	1411	N/A	-0.20	0.30	0.2	0.4	43.16	5.58	La Ciotat-Hyères	L. byssoides	N/A	12	23	*
115	LGQ-769	N/A	N/A	439	170	99	779	N/A	-0.50	0.40	0.4	0.4	43.16	5.58	La Ciotat-Hyères	L. byssoides	N/A	12	23	*
116	LGQ-768	N/A	N/A	-618	188	-994	-242	N/A	-0.90	0.40	0.4	0.4	43.16	5.58	La Ciotat-Hyères	L. byssoides	N/A	12	23	*
117	LGQ-764	N/A	N/A	-1028	182	-1392	-664	N/A	-1.00	0.40	0.4	0.4	43.16	5.58	La Ciotat-Hyères	L. byssoides	N/A	12	23	*
118	LGQ-770	N/A	N/A	-1088	177	-1442	-734	N/A	-1.00	0.40	0.4	0.4	43.16	5.58	La Ciotat-Hyères	L. byssoides	N/A	12	23	*

119	LGQ-765	N/A	N/A	-2194	236	-2666	-1722	N/A	-1.30	0.40	0.4	0.4	43.16	5.58	La Ciotat-Hyères	L. byssoides	N/A	12	23	*
120	LGQ-766	N/A	N/A	-1435	172	-1779	-1091	N/A	-1.30	0.40	0.4	0.4	43.16	5.58	La Ciotat-Hyères	L. byssoides	N/A	12	23	*
121	LGQ-767	N/A	N/A	-1689	187	-2063	-1315	N/A	-1.40	0.40	0.4	0.4	43.16	5.58	La Ciotat-Hyères	L. byssoides	N/A	12	23	*
122	LGQ-682	N/A	N/A	268	137	-6	542	N/A	-0.50	0.40	0.4	0.4	43.03	6.1	La Ciotat-Hyères	L. byssoides	N/A	12	23	*
123	LGQ-683	N/A	N/A	-244	151	-546	58	N/A	-0.70	0.40	0.4	0.4	43.03	6.1	La Ciotat-Hyères	L. byssoides	N/A	12	23	*
124	LGQ-684	N/A	N/A	-477	272	-1021	67	N/A	-0.90	0.40	0.4	0.4	43.03	6.1	La Ciotat-Hyères	L. byssoides	N/A	12	23	*
125	LGQ-829	N/A	N/A	-907	112	-1131	-683	N/A	-0.90	0.40	0.4	0.4	43.01	6.38	La Ciotat-Hyères	L. byssoides	N/A	12	23	*
126	LGQ-826	N/A	N/A	-720	180	-1080	-360	N/A	-1.10	0.40	0.4	0.4	43.01	6.38	La Ciotat-Hyères	L. byssoides	N/A	12	23	*
127	Esc-1.19	N/A	N/A	-670	126	-922	-418	N/A	-0.50	0.60	0.6	0.6	43.43	6.7	Frejus	Grains	N/A	13	29	*
128	POZ-14371	N/A	N/A	-119	146	-411	173	N/A	-0.40	0.30	0.3	0.3	43.43	6.73	Frejus	Shell	N/A	13	30	*
129	POZ-14372	N/A	N/A	-155	151	-457	147	N/A	-0.40	0.30	0.3	0.3	43.43	6.73	Frejus	Shell	N/A	13	30	*
130	POZ-24339	N/A	N/A	507	111	285	729	N/A	-0.40	0.30	0.3	0.3	43.43	6.73	Frejus	Shell	N/A	13	31	*
131	LY-9154	N/A	N/A	564	106	352	776	N/A	-0.30	0.30	0.3	0.3	43.43	6.73	Frejus	Shell	N/A	13	31	*
132	N/A	N/A	N/A	35	35	-35	105	N/A	-0.50	0.20	0.2	0.2	43.43	6.73	Frejus	hells on fishtar	N/A	13	31	*
133	LGQ- 703	N/A	N/A	-473	272	-1017	71	N/A	-0.50	0.40	0.4	0.4	43.41	6.85	Frejus-Dramont	L. byssoides	N/A	13	23	*
134	LGQ- 697	N/A	N/A	-967	153	-1273	-661	N/A	-0.90	0.40	0.4	0.4	43.41	6.85	Frejus-Dramont	L. byssoides	N/A	13	23	*
135	LGQ- 859	N/A	N/A	755	122	511	999	N/A	-0.20	0.40	0.4	0.4	43.67	7.32	Cap-Ferrat	L. byssoides	N/A	14	23	*
136	Poz-11380	N/A	N/A	-4090	132	-4354	-3826	N/A	-4.80	1.00	1	1	43.83	10.33	Versilia	Charcoal	N/A	15	32	*
137	Poz-11381	N/A	N/A	-4175	131	-4437	-3913	N/A	-4.90	1.00	1	1	43.83	10.33	Versilia	-	N/A	15	32	*
138	Poz-11382	N/A	N/A	-4190	136	-4462	-3918	N/A	-5.00	1.00	1	1	43.83	10.33	Versilia	Bark	N/A	15	32	*
139	Poz-10665	N/A	N/A	-4829	103	-5035	-4623	N/A	-6.40	0.60	0.6	0.6	43.83	10.33	Versilia	Charcoal	N/A	15	32	*
140	N/A	N/A	N/A	-255	139	-533	23	N/A	-1.00	0.60	0.6	0.6	43.81	10.34	Versilia	Organics	N/A	15	33	*
141	N/A	N/A	N/A	-2300	156	-2612	-1988	N/A	-2.10	0.60	0.6	0.6	43.81	10.34	Versilia	Wood	N/A	15	33	*
142	N/A	N/A	N/A	-2662	174	-3010	-2314	N/A	-2.20	0.60	0.6	0.6	43.81	10.34	Versilia	Shell	N/A	15	33	*
143	N/A	N/A	N/A	-5493	119	-5731	-5255	N/A	-9.00	0.60	0.6	0.6	43.81	10.34	Versilia	Shell	N/A	15	33	*
144	N/A	N/A	N/A	-8458	182	-8822	-8094	N/A	-34.00	0.70	0.7	0.7	43.81	10.34	Versilia	Shell	N/A	15	33	*
145	N/A	N/A	N/A	-5991	87	-6165	-5817	N/A	-10.00	0.80	0.8	0.8	43.81	10.34	Versilia	Shell	N/A	15	33	*
146	N/A	N/A	N/A	-5838	147	-6132	-5544	N/A	-12.50	1.00	1	1	43.73	10.43	Versilia	Shell	N/A	15	33	*
147	N/A	N/A	N/A	-4206	206	-4618	-3794	N/A	-4.70	1.00	1	1	43.7	10.3	Versilia	Shell	N/A	15	33	*
148	N/A	N/A	N/A	1258	34	1190	1326	N/A	0.00	0.25	0	0.5	43.7	10.3	Portus Pisanus	Seed	N/A	15	34	
149	N/A	N/A	N/A	-3660	172	-4004	-3316	N/A	-3.30	0.60	0.6	0.6	43.7	10.3	Portus Pisanus	Shell	N/A	15	34	
150	N/A	N/A	N/A	-3193	154	-3501	-2885	N/A	-2.60	0.60	0.6	0.6	43.7	10.3	Portus Pisanus	Seed	N/A	15	34	
151	LGQ- 835	N/A	N/A	967	188	591	1343	N/A	-0.30	0.35	0.3	0.4	43.02	9.4	Cap Corse	L. byssoides	N/A	16	23	*
152	LGQ- 836	N/A	N/A	-477	272	-1021	67	N/A	-0.80	0.40	0.4	0.4	43.02	9.4	Cap Corse	L. byssoides	N/A	16	23	*
153	LGQ- 837	N/A	N/A	-758	211	-1180	-336	N/A	-0.90	0.40	0.4	0.4	43.02	9.4	Cap Corse	L. byssoides	N/A	16	23	*
154	LGQ- 838	N/A	N/A	-1365	139	-1643	-1087	N/A	-1.10	0.40	0.4	0.4	43.02	9.4	Cap Corse	L. byssoides	N/A	16	23	*
155	LGQ- 839	N/A	N/A	316	188	-60	692	N/A	-0.40	0.40	0.4	0.4	42.96	9.34	Cap Corse	L. byssoides	N/A	16	23	*
156	LGQ- 840	N/A	N/A	1161	118	925	1397	N/A	-0.60	0.40	0.4	0.4	42.96	9.34	Cap Corse	L. byssoides	N/A	16	23	*
157	LGQ- 841	N/A	N/A	-1194	197	-1588	-800	N/A	-1.00	0.40	0.4	0.4	42.96	9.34	Cap Corse	L. byssoides	N/A	16	23	*
158	LGQ- 842	N/A	N/A	-1940	193	-2326	-1554	N/A	-1.10	0.40	0.4	0.4	42.96	9.34	Cap Corse	L. byssoides	N/A	16	23	*
159	LGQ- 843	N/A	N/A	-1812	198	-2208	-1416	N/A	-1.30	0.40	0.4	0.4	42.96	9.34	Cap Corse	L. byssoides	N/A	16	23	*
160	LGQ- 832	N/A	N/A	551	123	305	797	N/A	-0.40	0.40	0.4	0.4	42.37	8.54	Scandola	L. byssoides	N/A	17	23	*
161	LGQ- 834	N/A	N/A	-455	271	-997	87	N/A	-0.60	0.40	0.4	0.4	42.37	8.54	Scandola	L. byssoides	N/A	17	23	*
162	LGQ- 833	N/A	N/A	-1573	160	-1893	-1253	N/A	-1.10	0.40	0.4	0.4	42.37	8.54	Scandola	L. byssoides	N/A	17	23	*
163	LGQ- 862	N/A	N/A	-2041	158	-2357	-1725	N/A	-1.60	0.40	0.4	0.4	42.37	8.54	Scandola	L. byssoides	N/A	17	23	*
164	LGQ- 861	N/A	N/A	297	209	-121	715	N/A	-0.50	0.40	0.4	0.4	42.37	8.54	Scandola	L. byssoides	N/A	17	23	*
165	LGQ- 864	N/A	N/A	-197	198	-593	199	N/A	-0.80	0.40	0.4	0.4	42.37	8.54	Scandola	L. byssoides	N/A	17	23	*
166	Poz-65992	N/A	N/A	-317	87	-491	-143	N/A	-0.40	0.45	0.4	0.5	42.11	8.69	Sagone	Plant remains	N/A	18	35	**
167	Poz-65994	N/A	N/A	-458	76	-610	-306	N/A	-0.40	0.45	0.4	0.5	42.11	8.69	Sagone	Plant remains	N/A	18	35	**
168	Poz-65995	N/A	N/A	-298	93	-484	-112	N/A	-0.80	0.50	0.5	0.5	42.11	8.69	Sagone	Plant remains	N/A	18	35	**
169	Poz-58646	N/A	N/A	1261	37	1187	1335	N/A	-0.30	0.40	0.3	0.5	42.11	8.69	Sagone	Plant remains	N/A	18	35	**
170	Poz-58648	N/A	N/A	634	35	564	704	N/A	-0.40	0.45	0.4	0.5	42.11	8.69	Sagone	Plant remains	N/A	18	35	**
171	Poz-58650	N/A	N/A	47	89	-131	225	N/A	-0.60	0.50	0.5	0.5	42.11	8.69	Sagone	Plant remains	N/A	18	35	**
172	Poz-58651	N/A	N/A	398	134	130	666	N/A	-0.70	0.50	0.5	0.5	42.11	8.69	Sagone	Plant remains	N/A	18	35	**
173	Poz-65998	N/A	N/A	1737	213	1311	2163	N/A	-0.40	0.45	0.4	0.5	42.11	8.69	Sagone	Organics	N/A	18	35	**
174	Poz-65996	N/A	N/A	1246	36	1174	1318	N/A	-0.50	0.50	0.5	0.5	42.11	8.69	Sagone	Plant remains	N/A	18	35	**
175	Poz-65925	N/A	N/A	-240	119	-478	-2	N/A	-1.20	0.50	0.5	0.5	42.11	8.69	Sagone	Organics	N/A	18	35	**
176	Poz-58642	N/A	N/A	1105	77	951	1259	N/A	-0.60	0.50	0.5	0.5	42.11	8.69	Sagone	Wood	N/A	18	35	**
177	Poz-55976	N/A	N/A	884	105	674	1094	N/A	-1.70	0.50	0.5	0.5	42.11	8.69	Sagone	Wood	N/A	18	35	**
178	Beta-450507	N/A	N/A	-1520	121	-1762	-1278	N/A	-2.00	0.50	0.5	0.5	41.72	8,809	Tanghiccia	Shell	N/A	19	36	**

179	Poz-82975	N/A	N/A	-1581	76	-1733	-1429	N/A	-1.70	1.00	1	1	41.72	8,809	Tanghiccia	Wood	N/A	19	36	**
180	Poz-56332	N/A	N/A	-1521	87	-1695	-1347	N/A	-1.80	1.00	1	1	41.72	8,809	Tanghiccia	Plant remains	N/A	19	36	**
181	Poz-82974	N/A	N/A	-1587	78	-1743	-1431	N/A	-2.00	1.00	1	1	41.72	8,809	Tanghiccia	Peat	N/A	19	36	**
182	Poz-87300	N/A	N/A	-1684	147	-1978	-1390	N/A	-2.00	1.00	1	1	41.72	8,809	Tanghiccia	Shell	N/A	19	36	**
183	Poz-71368	N/A	N/A	1142	108	926	1358	N/A	-0.10	0.30	0.1	0.5	42.09	9.52	Sale	Shell	N/A	20	37	**
184	Poz-65452	N/A	N/A	-555	160	-875	-235	N/A	-0.40	0.45	0.4	0.5	42.09	9.52	Sale	Shell	N/A	20	37	**
185	Poz-65838	N/A	N/A	-2126	142	-2410	-1842	N/A	-0.80	0.50	0.5	0.5	42.09	9.52	Sale	Charcoal	N/A	20	37	**
186	Poz-65450	N/A	N/A	-2229	170	-2569	-1889	N/A	-1.20	0.50	0.5	0.5	42.09	9.52	Sale	Shell	N/A	20	37	**
187	Poz-65451	N/A	N/A	-2260	166	-2592	-1928	N/A	-1.20	0.50	0.5	0.5	42.09	9.52	Sale	Shell	N/A	20	37	**
188	N/A	N/A	N/A	-2669	183	-3035	-2303	N/A	-1.90	0.50	0.5	0.5	42.09	9.52	Sale	Charcoal	N/A	20	37	**
189	Poz-65453	N/A	N/A	-3221	152	-3525	-2917	N/A	-2.70	0.50	0.5	0.5	42.09	9.52	Sale	Shell	N/A	20	37	**
190	Poz-65449	N/A	N/A	-3409	131	-3671	-3147	N/A	-3.80	0.60	0.6	0.6	42.09	9.52	Sale	Shell	N/A	20	37	**
191	Poz-66301	N/A	N/A	-1659	99	-1857	-1461	N/A	-0.80	0.90	0.8	1	41.37	9.26	Bonifacio Strait	Organics	N/A	21	38	**
192	Poz-66301	N/A	N/A	-2545	73	-2691	-2399	N/A	-1.80	0.50	0.5	0.5	41.37	9.26	Bonifacio Strait	Organics	N/A	21	38	**
193	Poz-77841	N/A	N/A	-455	77	-609	-301	N/A	-0.70	0.60	0.6	0.6	41.28	9.35	Bonifacio Strait	Organics	N/A	21	38	**
194	Poz-77844	N/A	N/A	-1414	87	-1588	-1240	N/A	-1.30	0.60	0.6	0.6	41.28	9.35	Bonifacio Strait	Organics	N/A	21	38	**
195	Poz-77842	N/A	N/A	1642	149	1344	1940	N/A	-0.80	0.60	0.6	0.6	41.28	9.35	Bonifacio Strait	Organics	N/A	21	38	**
196	N/A	N/A	N/A	523	124	275	771	N/A	-0.40	0.70	0.4	1	42.43	11.17	Orbetello	Shell	N/A	22	39	
197	N/A	N/A	N/A	0	50	-100	100	N/A	-0.90	0.40	0.4	0.4	42.43	11.15	Orbetello	Fishtank	N/A	22	40	
198	N/A	N/A	N/A	0	50	-100	100	N/A	-1.00	0.60	0.6	0.6	42.03	11.86	S. Marinella Gr.	Fishtank	N/A	23	40	
199	N/A	N/A	N/A	0	50	-100	100	N/A	-0.90	0.50	0.5	0.5	42.03	11.9	Marinella Od.	Fishtank	N/A	23	40	
200	N/A	N/A	N/A	0	50	-100	100	N/A	-0.90	0.40	0.4	0.4	42	11.82	Punta della Vipera	Fishtank	N/A	23	40	
201	R-1198 a	N/A	N/A	-3502	132	-3766	-3238	N/A	-2.60	1.20	1.2	1.2	41.84	12.26	Tiber delta	Peaty clay	N/A	24	42	*
202	R-1198	N/A	N/A	-3508	135	-3778	-3238	N/A	-2.60	1.20	1.2	1.2	41.84	12.26	Tiber delta	Peaty clay	N/A	24	42	*
203	R-888	N/A	N/A	-6589	161	-6911	-6267	N/A	-8.80	1.20	1.2	1.2	41.84	12.26	Tiber delta	Organics	N/A	24	42	*
204	R-1199	N/A	N/A	-4099	131	-4361	-3837	N/A	-3.60	1.20	1.2	1.2	41.84	12.26	Tiber delta	Organics	N/A	24	42	*
205	R-1200	N/A	N/A	-8988	215	-9418	-8558	N/A	-28.00	1.50	1.5	1.5	41.84	12.26	Tiber delta	Organics	N/A	24	42	*
206	R-1200 A/a	N/A	N/A	-8980	248	-9476	-8484	N/A	-28.00	1.50	1.5	1.5	41.84	12.26	Tiber delta	Wood	N/A	24	42	*
207	R-1198a	N/A	N/A	-3502	132	-3766	-3238	N/A	-2.10	1.20	1.2	1.2	41.83	12.26	Tiber delta	Peat	N/A	24	42	*
208	R-1198	N/A	N/A	-3508	135	-3778	-3238	N/A	-2.10	1.20	1.2	1.2	41.83	12.26	Tiber delta	Peat	N/A	24	42	*
209	R-887a	N/A	N/A	-3369	265	-3899	-2839	N/A	-3.10	1.20	1.2	1.2	41.83	12.26	Tiber delta	Wood	N/A	24	42	*
210	R-1623	N/A	N/A	-4099	131	-4361	-3837	N/A	-3.10	1.20	1.2	1.2	41.83	12.26	Tiber delta	Wood	N/A	24	42	*
211	R-1624	N/A	N/A	-3372	259	-3890	-2854	N/A	-2.10	1.20	1.2	1.2	41.83	12.26	Tiber delta	Organics	N/A	24	42	*
212	R-1200	N/A	N/A	-8988	215	-9418	-8558	N/A	-30.00	1.20	1.2	1.2	41.83	12.26	Tiber delta	Silt	N/A	24	42	*
213	R-1200a	N/A	N/A	-9103	266	-9635	-8571	N/A	-30.00	1.20	1.2	1.2	41.83	12.26	Tiber delta	Wood	N/A	24	43	*
214	LTL-1494A	N/A	N/A	61	149	-237	359	N/A	-0.60	0.60	0.6	0.6	41.83	12.27	Tiber delta	Bulk	N/A	24	43	*
215	LYON-8805	N/A	N/A	-7692	193	-8078	-7306	N/A	-12.30	1.00	1	1	41.82	12.28	Tiber delta	Shell	N/A	24	43	*
216	LYON-8806	N/A	N/A	-7620	177	-7974	-7266	N/A	-13.80	1.00	1	1	41.82	12.28	Tiber delta	Shell	N/A	24	43	*
217	LYON-8803	N/A	N/A	-7969	225	-8419	-7519	N/A	-15.30	1.00	1	1	41.82	12.28	Tiber delta	Shell	N/A	24	43	*
218	LYON-8785	N/A	N/A	-1460	49	-1558	-1362	N/A	-1.50	0.50	0.5	0.5	41.82	12.28	Tiber delta	Wood	N/A	24	43	*
219	LY-4198	N/A	N/A	239	162	-85	563	N/A	-0.80	0.20	0.2	0.2	41.78	12.25	Tiber delta	Shell in harbou	N/A	24	44	*
220	12	N/A	N/A	-8034	305	-8644	-7424	N/A	-33.50	1.60	1.6	1.6	40.44	9.78	Cala Liberotto	Beachrock	N/A	25	45	*
221	DSH6660	N/A	N/A	-4956	119	-5194	-4718	N/A	-5.50	1.30	1.3	1.3	40.64	9.73	Posada	Organics	N/A	25	46	**
222	DSH6666	N/A	N/A	-5335	121	-5577	-5093	N/A	-7.20	1.30	1.3	1.3	40.64	9.73	Posada	Organics	N/A	25	46	**
223	DSH6668	N/A	N/A	-5284	78	-5440	-5128	N/A	-4.60	1.30	1.3	1.3	40.64	9.73	Posada	Organics	N/A	25	46	**
224	DSH6664	N/A	N/A	-5290	72	-5434	-5146	N/A	-6.10	1.30	1.3	1.3	40.64	9.73	Posada	Organics	N/A	25	46	**
225	DSH6665	N/A	N/A	-5555	70	-5695	-5415	N/A	-7.40	1.30	1.3	1.3	40.64	9.73	Posada	Organics	N/A	25	46	**
226	DSH6667	N/A	N/A	-5387	81	-5549	-5225	N/A	-7.00	1.30	1.3	1.3	40.64	9.73	Posada	Organics	N/A	25	46	**
227	DSH6661	N/A	N/A	-5631	95	-5821	-5441	N/A	-9.70	1.30	1.3	1.3	40.64	9.73	Posada	Organics	N/A	25	46	**
228	DSH6611	N/A	N/A	1207	105	997	1417	N/A	-0.80	0.80	0.8	0.8	39.9	8.53	Gulf of Oristano	Organics	N/A	26	47	**
229	DSH6612	N/A	N/A	1091	67	957	1225	N/A	-2.00	0.80	0.8	0.8	39.9	8.53	Gulf of Oristano	Organics	N/A	26	47	**
230	DSH5650	N/A	N/A	-3933	136	-4205	-3661	N/A	-4.40	1.30	1.3	1.3	39.9	8.53	Gulf of Oristano	Organics	N/A	26	47	**
231	DSH5657	N/A	N/A	-5502	116	-5734	-5270	N/A	-6.20	1.30	1.3	1.3	39.9	8.53	Gulf of Oristano	Organics	N/A	26	47	**
232	DSH5659	N/A	N/A	-5730	121	-5972	-5488	N/A	-8.00	1.30	1.3	1.3	39.9	8.53	Gulf of Oristano	Organics	N/A	26	47	**
233	DSH5658	N/A	N/A	-4110	128	-4366	-3854	N/A	-4.00	1.30	1.3	1.3	39.9	8.53	Gulf of Oristano	Organics	N/A	26	47	**
234	DSH6610	N/A	N/A	-3464	159	-3782	-3146	N/A	-4.90	0.80	0.8	0.8	39.9	8.53	Gulf of Oristano	Organics	N/A	26	47	**
235	DSH5788	N/A	N/A	-3513	130	-3773	-3253	N/A	-5.90	0.80	0.8	0.8	39.9	8.53	Gulf of Oristano	Organics	N/A	26	47	**
236	DSH6541	N/A	N/A	-3594	68	-3730	-3458	N/A	-6.20	0.80	0.8	0.8	39.9	8.53	Gulf of Oristano	Organics	N/A	26	47	**
237	DSH6996_S	N/A	N/A	-3697	63	-3823	-3571	N/A	-3.60	0.80	0.8	0.8	39.9	8.53	Gulf of Oristano	Organics	N/A	26	47	**
238	DSH6997_S	N/A	N/A	-4115	112	-4339	-3891	N/A	-4.40	0.80	0.8	0.8	39.9	8.53	Gulf of Oristano	Organics	N/A	26	47	**

239	AA-92534	N/A	N/A	697	81	535	859	N/A	-0.30	0.65	0.3	1	39.89	8.45	Gulf of Oristano	Organics	N/A	26	48	**
240	AA-92535	N/A	N/A	-556	173	-902	-210	N/A	-1.40	1.00	1	1	39.89	8.45	Gulf of Oristano	Organics	N/A	26	48	**
241	AA-84428	N/A	N/A	-2660	189	-3038	-2282	N/A	-2.20	1.00	1	1	39.89	8.45	Gulf of Oristano	Organics	N/A	26	48	**
242	14V1	N/A	N/A	-7454	132	-7718	-7190	N/A	-27.00	1.10	1.1	1.1	39.81	8.45	Gulf of Oristano	Shell	N/A	26	49	**
243	P26-4	N/A	N/A	-245	114	-473	-17	N/A	-1.70	1.10	1.1	1.1	39.74	8.61	Gulf of Oristano	Shell	N/A	26	50	**
244	P26-3.45	N/A	N/A	-30	158	-346	286	N/A	-1.50	1.10	1.1	1.1	39.74	8.61	Gulf of Oristano	Shell	N/A	26	50	**
245	N/A	N/A	N/A	-300	100	-500	-100	N/A	-1.30	0.50	0.5	0.5	39.07	8.46	Sant'Antioco	rcheol. structu	N/A	27	51	**
246	N/A	N/A	N/A	60	20	20	100	N/A	-1.10	0.30	0.3	0.3	39.05	8.47	Sant'Antioco	mics in beach	N/A	27	51	**
247	LTL-8291A	N/A	N/A	134	165	-196	464	N/A	-0.20	0.60	0.2	1	38.9	8.8	Malfatano	Shell	N/A	28	52	**
248	LTL-8292A	N/A	N/A	-89	177	-443	265	N/A	-1.30	1.00	1	1	38.9	8.8	Malfatano	Shell	N/A	28	52	**
249	LTL-8293A	N/A	N/A	-1104	192	-1488	-720	N/A	-2.30	1.00	1	1	38.9	8.8	Malfatano	Shell	N/A	28	52	**
250	GX-29077	N/A	N/A	-7729	170	-8069	-7389	N/A	-29.50	1.00	1	1	39.21	9.09	Cagliari plain	Shell	N/A	29	53	**
251	GX-25487	N/A	N/A	-8891	251	-9393	-8389	N/A	-45.50	1.60	1.6	1.6	39.21	9.09	Cagliari plain	Shell	N/A	29	53	**
252	N/A	N/A	N/A	0	50	-100	100	N/A	-0.90	0.40	0.4	0.4	41.25	13.6	Sarinola	Fishtanks	N/A	30	40	
253	CV-10	N/A	N/A	-2579	285	-3149	-2009	N/A	-2.50	0.60	0.6	0.6	40.97	14	Volturno	Wood	N/A	30	54	*
254	CV-5	N/A	N/A	-5567	96	-5759	-5375	N/A	-7.50	0.60	0.6	0.6	40.97	14	Volturno	Wood	N/A	30	54	*
255	G1bis 5/41	N/A	N/A	-163	198	-559	233	N/A	-1.00	0.50	0.5	0.5	40.94	14.03	Volturno	Shell	N/A	30	55	*
256	ROME-665	N/A	N/A	-7305	221	-7747	-6863	N/A	-14.70	1.10	1.1	1.1	40.42	15	Salerno Bay	Organics	N/A	31	56	*
257	ROME-666	N/A	N/A	-7379	192	-7763	-6995	N/A	-16.30	1.10	1.1	1.1	40.42	15	Salerno Bay	Wood debris	N/A	31	56	*
258	N/A	N/A	N/A	-5269	262	-5793	-4745	N/A	-3.20	1.10	1.1	1.1	40.39	15	Salerno Bay	Foraminifera	N/A	31	57	*
259	N/A	N/A	N/A	-2150	50	-2250	-2050	N/A	-0.50	1.10	1.1	1.1	40.39	15	Salerno Bay	Tephra layer	N/A	31	57	*
260	N/A	N/A	N/A	-6253	196	-6645	-5861	N/A	-9.80	1.10	1.1	1.1	40.39	15	Salerno Bay	Shell	N/A	31	57	*
261	N/A	N/A	N/A	-6442	193	-6828	-6056	N/A	-8.30	1.10	1.1	1.1	40.39	15	Salerno Bay	Shell	N/A	31	57	*
262	Rome-815	N/A	N/A	507	117	273	741	N/A	-1.50	0.70	0.7	0.7	40.49	14.94	Salerno Bay	Organics	N/A	31	58	
263	Rome-811	N/A	N/A	-2081	194	-2469	-1693	N/A	-4.50	0.70	0.7	0.7	40.49	14.94	Salerno Bay	Organics	N/A	31	58	
264	Rome-816	N/A	N/A	-7371	195	-7761	-6981	N/A	-7.50	0.55	0	1.1	40.49	14.94	G. of Gaeta-Volturno	Organics	N/A	31	58	
265	R-2580	N/A	N/A	1583	111	1361	1805	N/A	-0.40	0.30	0.3	0.3	38.21	13.28	SanVito- C.Gallo	Vermetid	N/A	32	59	*
266	R-2764	N/A	N/A	1830	121	1588	2072	N/A	-0.30	0.30	0.3	0.3	38.11	12.71	SanVito- C.Gallo	Vermetid	N/A	32	59	*
267	R-2741	N/A	N/A	1835	115	1605	2065	N/A	-0.30	0.30	0.3	0.3	38.17	12.71	SanVito- C.Gallo	Vermetid	N/A	32	59	*
268	R-2742	N/A	N/A	1835	115	1605	2065	N/A	-0.30	0.30	0.3	0.3	38.17	12.71	SanVito- C.Gallo	Vermetid	N/A	32	59	*
269	OZE-613	N/A	N/A	-851	140	-1131	-571	N/A	-1.10	0.60	0.6	0.6	37.89	12.45	MarsalaSound	Shell	N/A	33	60	*
270	OZE-612	N/A	N/A	-549	175	-899	-199	N/A	-0.40	0.50	0.4	0.6	37.89	12.45	MarsalaSound	Shell	N/A	33	60	*
271	OZE-611	N/A	N/A	1199	139	921	1477	N/A	-0.20	0.40	0.2	0.6	37.87	12.48	MarsalaSound	Shell	N/A	33	60	*
272	OZE-610	N/A	N/A	1672	156	1360	1984	N/A	-0.10	0.35	0.1	0.6	37.84	12.45	MarsalaSound	Shell	N/A	33	60	*
273	OZE-609	N/A	N/A	903	141	621	1185	N/A	-0.10	0.35	0.1	0.6	37.87	12.45	MarsalaSound	Shell	N/A	33	60	*
274	POZ-17907	N/A	N/A	-2696	192	-3080	-2312	N/A	-4.40	1.10	1.1	1.1	36.8	15.09	Vendicari-Pachino	Shell	N/A	34	61	*
275	POZ-17906	N/A	N/A	-3097	202	-3501	-2693	N/A	-5.90	1.10	1.1	1.1	36.8	15.09	Vendicari-Pachino	Shell	N/A	34	61	*
276	LTL4282A	N/A	N/A	528	153	222	834	N/A	0.00	0.55	0	1.1	36.7	15.11	Vendicari-Pachino	Shell	N/A	34	62	*
277	LTL4284A	N/A	N/A	579	159	261	897	N/A	0.00	0.55	0	1.1	36.7	15.11	Vendicari-Pachino	Shell	N/A	34	62	*
278	LTL4285A	N/A	N/A	-1992	210	-2412	-1572	N/A	-2.10	1.10	1.1	1.1	36.7	15.11	Vendicari-Pachino	Shell	N/A	34	62	*
279	LTL4887A	N/A	N/A	423	188	47	799	N/A	-0.40	0.75	0.4	1.1	36.7	15.1	Vendicari-Pachino	Shell	N/A	34	62	*
280	LTL4888A	N/A	N/A	-2874	234	-3342	-2406	N/A	-3.20	1.10	1.1	1.1	36.7	15.1	Vendicari-Pachino	Shell	N/A	34	62	*
281	LTL4889A	N/A	N/A	1829	121	1587	2071	N/A	0.00	0.55	0	1.1	36.7	15.1	Vendicari-Pachino	Shell	N/A	34	62	*
282	LTL4903A	N/A	N/A	-935	163	-1261	-609	N/A	-1.80	1.10	1.1	1.1	36.7	15.1	Vendicari-Pachino	Shell	N/A	34	62	*
283	POZ-42441	N/A	N/A	-4211	136	-4483	-3939	N/A	-7.00	1.00	1	1	35.93	14.41	Malta	Charcoal	N/A	35	63	*
284	SACA-11668	N/A	N/A	-5077	129	-5335	-4819	N/A	-9.20	0.70	0.7	0.7	35.93	14.41	Malta	Peat	N/A	35	63	*
285	SACA-11669	N/A	N/A	-5449	73	-5595	-5303	N/A	-9.60	0.50	0.5	0.5	35.93	14.41	Malta	Charcoal	N/A	35	63	*
286	POZ-42439	N/A	N/A	-5571	88	-5747	-5395	N/A	-11.10	1.00	1	1	35.93	14.41	Malta	Charcoal	N/A	35	63	*
287	POZ-42444	N/A	N/A	-4946	99	-5144	-4748	N/A	-8.20	1.00	1	1	35.93	14.41	Malta	Charcoal	N/A	35	63	*
288	LTL14449A3	N/A	N/A	-5677	56	-5789	-5565	N/A	-14.80	0.50	0.5	0.5	35.84	14.396	Malta	Speleothem	N/A	35	64	*
289	N/A	N/A	N/A	-3511	175	-3861	-3161	N/A	0.50	1.10	1.1	1.1	34.2	10.03	ElGuettate-Dreiaa	Shell	N/A	36	65	*
290	N/A	N/A	N/A	-5502	257	-6016	-4988	N/A	-0.60	0.90	0.9	0.9	34.2	10.03	ElGuettate-Dreiaa	Shell	N/A	36	65	*
291	N/A	N/A	N/A	-3467	182	-3831	-3103	N/A	0.20	0.70	0.7	0.7	34.2	10.03	ElGuettate-Dreiaa	Shell	N/A	36	65	*
292	SACA-12307	N/A	N/A	1304	131	1042	1566	N/A	0.40	0.70	0.7	0.7	34.17	10.02	ElGuettate-Dreiaa	Shell	N/A	36	66	*
293	SACA-12306	N/A	N/A	1192	144	904	1480	N/A	0.70	0.70	0.7	0.7	34.17	10.02	ElGuettate-Dreiaa	Shell	N/A	36	66	*
294	BETA-282579	N/A	N/A	-4721	201	-5123	-4319	N/A	0.10	1.10	1.1	1.1	34.16	10.01	ElGuettate-Dreiaa	Shell	N/A	36	66	*
295	POZ-2590	N/A	N/A	-2344	211	-2766	-1922	N/A	0.40	0.80	0.8	0.8	33.73	10.72	Humt	Shell	N/A	37	67	*
296	LU-2656	N/A	N/A	-1343	224	-1791	-895	N/A	-0.30	0.80	0.8	0.8	33.3	11.12	ElBibane-Boujmel	eachrock ceme	N/A	38	68	*
297	LU-2653	N/A	N/A	-1185	225	-1635	-735	N/A	-0.40	0.80	0.8	0.8	33.3	11.12	ElBibane-Boujmel	eachrock ceme	N/A	38	68	*
298	LU-2652	N/A	N/A	-2550	273	-3096	-2004	N/A	0.00	0.80	0.8	0.8	33.3	11.12	ElBibane-Boujmel	eachrock ceme	N/A	38	68	*

299	N/A	N/A	N/A	155	255	-355	665	N/A	0.40	0.60	0.6	0.6	33.29	11.09	ElBibane-Boujmel	Bulk material	N/A	38	69	*
300	N/A	N/A	N/A	-567	624	-1815	681	N/A	0.20	0.60	0.6	0.6	33.29	11.09	ElBibane-Boujmel	Bulk material	N/A	38	69	*
301	N/A	N/A	N/A	-1208	291	-1790	-626	N/A	0.00	0.60	0.6	0.6	33.29	11.09	ElBibane-Boujmel	Bulk material	N/A	38	69	*
302	N/A	N/A	N/A	-2160	462	-3084	-1236	N/A	-0.10	0.60	0.6	0.6	33.29	11.09	ElBibane-Boujmel	Bulk material	N/A	38	69	*
303	N/A	N/A	N/A	-2362	466	-3294	-1430	N/A	-0.10	0.60	0.6	0.6	33.29	11.09	ElBibane-Boujmel	Bulk material	N/A	38	69	*
304	N/A	N/A	N/A	-4878	415	-5708	-4048	N/A	-0.30	0.60	0.6	0.6	33.29	11.09	ElBibane-Boujmel	Bulk material	N/A	38	69	*
305	ROME-1205	N/A	N/A	1359	66	1227	1491	N/A	-1.10	0.50	0.5	0.5	45.4	12.25	Venice lagoon	Bulk material	N/A	39	70	*
306	OZG-805	N/A	N/A	1168	110	948	1388	N/A	-0.70	0.60	0.6	0.6	45.35	12.32	Venice lagoon	Bulk material	N/A	39	70	*
307	OxA-10717	N/A	N/A	1138	102	934	1342	N/A	-1.60	1.20	1.2	1.2	45.47	12.41	Venice lagoon	Plant remains	N/A	39	71	*
308	OZ-G311	N/A	N/A	1021	126	769	1273	N/A	-0.90	0.60	0.6	0.6	45.48	12.33	Venice lagoon	Shell	N/A	39	70	*
309	OZG-332	N/A	N/A	689	199	291	1087	N/A	-0.40	0.70	0.4	1	45.35	12.32	Venice lagoon	Shell	N/A	39	70	*
310	OxA-10722	N/A	N/A	487	84	319	655	N/A	-0.70	0.95	0.7	1.2	45.47	12.41	Venice lagoon	Plant remains	N/A	39	71	*
311	OZ-G317	N/A	N/A	419	211	-3	841	N/A	-0.30	0.70	0.3	1.1	45.49	12.35	Venice lagoon	Shell	N/A	39	70	*
312	OZG-320	N/A	N/A	271	212	-153	695	N/A	-1.10	0.60	0.6	0.6	45.36	12.25	Venice lagoon	Shell	N/A	39	70	*
313	OxA-6784	N/A	N/A	254	127	0	508	N/A	-0.60	0.65	0.6	0.7	45.47	12.41	Venice lagoon	Wood	N/A	39	72	*
314	OZF-487	N/A	N/A	210	126	-42	462	N/A	-1.40	1.20	1.2	1.2	45.47	12.41	Venice lagoon	Plant remains	N/A	39	71	*
315	OZG-333	N/A	N/A	144	217	-290	578	N/A	-0.70	0.85	0.7	1	45.35	12.32	Venice lagoon	Shell	N/A	39	70	*
316	OxA-8629	N/A	N/A	126	100	-74	326	N/A	-0.90	0.70	0.7	0.7	45.47	12.41	Venice lagoon	Leaf	N/A	39	72	*
317	OZ-E696	N/A	N/A	-97	198	-493	299	N/A	-1.00	0.70	0.7	0.7	45.47	12.41	Venice lagoon	Foraminifera	N/A	39	72	*
318	LTL-1631A	N/A	N/A	-553	191	-935	-171	N/A	-1.40	0.60	0.6	0.6	45.47	12.29	Venice lagoon	Peat	N/A	39	73	*
319	OZG-322	N/A	N/A	-634	233	-1100	-168	N/A	-1.40	0.70	0.7	0.7	45.35	12.32	Venice lagoon	Foraminifera	N/A	39	70	*
320	CARG-12	N/A	N/A	-1143	122	-1387	-899	N/A	-0.90	1.05	0.9	1.2	45.54	12.44	Venice lagoon	-	N/A	39	74	*
321	OZ-E697	N/A	N/A	-1611	187	-1985	-1237	N/A	-2.20	0.70	0.7	0.7	45.47	12.41	Venice lagoon	Shell	N/A	39	72	*
322	OZ-E698	N/A	N/A	-1685	188	-2061	-1309	N/A	-2.20	0.70	0.7	0.7	45.47	12.41	Venice lagoon	Foraminifera	N/A	39	72	*
323	OZF-484	N/A	N/A	-2125	342	-2809	-1441	N/A	-2.00	1.20	1.2	1.2	45.47	12.41	Venice lagoon	Plant remains	N/A	39	71	*
324	OZ-E699	N/A	N/A	-2239	207	-2653	-1825	N/A	-1.80	0.70	0.7	0.7	45.47	12.41	Venice lagoon	Foraminifera	N/A	39	72	*
325	OxA-1076	N/A	N/A	-2300	157	-2614	-1986	N/A	-1.00	1.10	1	1.2	45.47	12.41	Venice lagoon	Plant remains	N/A	39	71	*
326	GX-26939	N/A	N/A	-2723	147	-3017	-2429	N/A	-4.30	0.80	0.8	0.8	45.48	12.41	Venice lagoon	Peat	N/A	39	71	*
327	OZF-080	N/A	N/A	-3606	237	-4080	-3132	N/A	-3.00	0.60	0.6	0.6	45.43	12.45	Venice lagoon	Shell	N/A	39	75	*
328	B6 Paris Sud	N/A	N/A	-4550	386	-5322	-3778	N/A	-5.50	0.70	0.7	0.7	45.67	12.93	Friuli lagoons	Organics	N/A	40	76	*
329	Ua-24876	N/A	N/A	-4577	75	-4727	-4427	N/A	-4.70	0.70	0.7	0.7	45.64	12.93	Friuli lagoons	Peat	N/A	40	77	*
330	Beta-184251	N/A	N/A	-5006	209	-5424	-4588	N/A	-9.00	0.80	0.8	0.8	45.63	12.88	Friuli lagoons	Peat	N/A	40	77	*
331	Ua-24049	N/A	N/A	-5547	75	-5697	-5397	N/A	-9.30	0.80	0.8	0.8	45.62	12.75	Friuli lagoons	Peat	N/A	40	78	*
332	ParisS-4209	N/A	N/A	329	320	-311	969	N/A	-0.60	0.60	0.6	0.6	45.62	12.95	Friuli lagoons	Shell	N/A	40	76	*
333	Beta-168127	N/A	N/A	-5462	77	-5616	-5308	N/A	-6.50	0.90	0.9	0.9	45.6	12.64	Friuli lagoons	Peat	N/A	40	79	*
334	Beta-157974	N/A	N/A	-1398	101	-1600	-1196	N/A	-3.40	0.60	0.6	0.6	45.58	12.47	Friuli lagoons	Peat	N/A	40	79	*
335	N/A	N/A	N/A	50	50	-50	150	N/A	-1.10	0.70	0.7	0.7	45.57	12.44	Friuli lagoons	eological struc	N/A	40	79	*
336	Beta-170844	N/A	N/A	-1933	199	-2331	-1535	N/A	-1.90	0.80	0.8	0.8	45.65	12.64	Friuli lagoons	Peat Organics	N/A	40	79	*
337	DSH-869	N/A	N/A	13	53	-93	119	N/A	-1.00	1.05	1	1.1	45.77	13.57	Gulf of Trieste	Wood	N/A	41	80	*
338	DSH-815	N/A	N/A	1086	115	856	1316	N/A	-0.70	0.85	0.7	1	45.77	13.57	Gulf of Trieste	Shell	N/A	41	80	*
339	Anto 2	N/A	N/A	1401	79	1243	1559	N/A	0.00	0.50	0	1	45.77	13.57	Gulf of Trieste	Shell	N/A	41	80	*
340	Anto 4	N/A	N/A	1017	151	715	1319	N/A	0.00	0.50	0	1	45.77	13.57	Gulf of Trieste	Shell	N/A	41	80	*
341	GT1-200	N/A	N/A	-8369	93	-8555	-8183	N/A	-25.20	1.20	1.2	1.2	45.67	13.67	Gulf of Trieste	Organics	N/A	41	81	*
342	POZ-15854	N/A	N/A	208	125	-42	458	N/A	-0.10	0.45	0.1	0.8	45.64	13.76	Gulf of Trieste	Shell	N/A	41	82	*
343	POZ-15856	N/A	N/A	-1234	177	-1588	-880	N/A	-0.10	0.45	0.1	0.8	45.64	13.76	Gulf of Trieste	Shell	N/A	41	82	*
344	Core GT3-64	N/A	N/A	-7627	125	-7877	-7377	N/A	-25.20	1.10	1.1	1.1	45,607	13.52	Gulf of Trieste	Shell	N/A	41	81	*
345	N/A	N/A	N/A	1037	190	657	1417	N/A	-0.20	0.70	0.2	1.2	45.54	13.72	Gulf of Trieste	Shell	N/A	41	83	*
346	Core-V6	N/A	N/A	-7952	319	-8590	-7314	N/A	-25.00	1.20	1.2	1.2	45.52	13.52	Istria	Shell	N/A	42	83	*
347	POZ-15849	N/A	N/A	904	114	676	1132	N/A	-0.20	0.60	0.2	1	45.28	13.6	Istria	Shell	N/A	42	84	*
348	POZ-15850	N/A	N/A	-1054	141	-1336	-772	N/A	-1.30	1.00	1	1	45.28	13.6	Istria	Shell	N/A	42	84	*
349	POZ-15845	N/A	N/A	1329	83	1163	1495	N/A	-0.10	0.55	0.1	1	45.11	13.62	Istria	Shell	N/A	42	84	*
350	POZ-15846	N/A	N/A	-3063	177	-3417	-2709	N/A	-2.90	1.00	1	1	45.11	13.62	Istria	Shell	N/A	42	84	*
351	POZ-15847	N/A	N/A	-3051	170	-3391	-2711	N/A	-2.90	1.00	1	1	45.11	13.62	Istria	Shell	N/A	42	84	*
352	BETA-187	N/A	N/A	-7257	188	-7633	-6881	N/A	-20.20	0.90	0.9	0.9	44.84	12.13	Romagna shelf	Organics	N/A	43	85	*
353	N/A	N/A	N/A	-8815	325	-9465	-8165	N/A	-24.60	0.90	0.9	0.9	44.72	12.02	Romagna shelf	Peat	N/A	43	86	*
354	N/A	N/A	N/A	-8088	333	-8754	-7422	N/A	-23.40	0.80	0.8	0.8	44.63	12.07	Romagna shelf	Organics	N/A	43	86	*
355	N/A	N/A	N/A	-10115	311	-10737	-9493	N/A	-41.80	1.00	1	1	44.49	12.89	Romagna shelf	Peat	N/A	43	86	*
356	N/A	N/A	N/A	-10159	281	-10721	-9597	N/A	-41.70	1.00	1	1	44.49	12.89	Romagna shelf	Peat	N/A	43	86	*
357	OMA-187Mezz	N/A	N/A	-3102	221	-3544	-2660	N/A	-4.10	0.60	0.6	0.6	44.88	12.1	Romagna shelf	rganic sedime	N/A	43	85	*
358	ENEA-Bolog-	N/A	N/A	-4084	260	-4604	-3564	N/A	-7.60	0.80	0.8	0.8	44.3	12.25	Romagna shelf	Organic clay	N/A	43	85	*

359	LNL-Livermor	N/A	N/A	-4687	136	-4959	-4415	N/A	-8.20	1.40	1.4	1.4	44.23	12.36	Romagna shelf	Organic clay	N/A	43	85	*
360	ENEA-Bolog-	N/A	N/A	-5168	311	-5790	-4546	N/A	-8.30	1.50	1.5	1.5	44.6	11.92	Romagna shelf	Organic clay	N/A	43	85	*
361	ENEA-Bolog-	N/A	N/A	-5684	193	-6070	-5298	N/A	-10.60	0.80	0.8	0.8	44.3	12.25	Romagna shelf	Organic clay	N/A	43	85	*
362	ETH	N/A	N/A	-5953	367	-6687	-5219	N/A	-10.80	1.20	1.2	1.2	44.62	12.01	Romagna shelf	Shell	N/A	43	87	*
363	LYON-9044	N/A	N/A	1258	34	1190	1326	N/A	0.00	0.10	0	0.2	44.54	14.91	North Dalmatia	Charcoal	N/A	44	88	*
364	LYON-9045	N/A	N/A	1069	82	905	1233	N/A	0.00	0.35	0	0.7	44.54	14.91	North Dalmatia	Plant remains	N/A	44	88	*
365	LYON-9048	N/A	N/A	955	62	831	1079	N/A	0.00	0.30	0	0.6	44.54	14.91	North Dalmatia	Plant remains	N/A	44	88	*
366	LYON-9049	N/A	N/A	1098	84	930	1266	N/A	0.00	0.30	0	0.6	44.54	14.91	North Dalmatia	Plant remains	N/A	44	88	*
367	Z-4301	N/A	N/A	1348	70	1208	1488	N/A	-0.30	0.30	0.3	0.3	43.08	16.18	Vis-Bisevo	L. byssoides	N/A	45	89	*
368	Z-4302	N/A	N/A	1374	64	1246	1502	N/A	-0.30	0.30	0.3	0.3	43.08	16.18	Vis-Bisevo	L. byssoides	N/A	45	89	*
369	Z-4303	N/A	N/A	1707	244	1219	2195	N/A	-0.30	0.30	0.3	0.3	43.08	16.18	Vis-Bisevo	L. byssoides	N/A	45	89	*
370	Z-4848	N/A	N/A	1548	95	1358	1738	N/A	-0.30	0.30	0.3	0.3	43.08	16.18	Vis-Bisevo	L. byssoides	N/A	45	89	*
371	Z-4849	N/A	N/A	1336	74	1188	1484	N/A	-0.30	0.30	0.3	0.3	43.08	16.18	Vis-Bisevo	L. byssoides	N/A	45	89	*
372	Z-4850	N/A	N/A	1532	100	1332	1732	N/A	-0.30	0.30	0.3	0.3	43.08	16.18	Vis-Bisevo	L. byssoides	N/A	45	89	*
373	Z-4851	N/A	N/A	1550	90	1370	1730	N/A	-0.30	0.30	0.3	0.3	43.08	16.18	Vis-Bisevo	L. byssoides	N/A	45	89	*
374	Z-4852	N/A	N/A	1640	156	1328	1952	N/A	-0.30	0.30	0.3	0.3	43.08	16.18	Vis-Bisevo	L. byssoides	N/A	45	89	*
375	Z-4307	N/A	N/A	783	187	409	1157	N/A	-0.70	0.30	0.3	0.3	43.08	16.18	Vis-Bisevo	L. byssoides	N/A	45	89	*
376	Z-4308	N/A	N/A	776	105	566	986	N/A	-0.70	0.30	0.3	0.3	43.08	16.18	Vis-Bisevo	L. byssoides	N/A	45	89	*
377	Z-4309	N/A	N/A	548	115	318	778	N/A	-0.70	0.30	0.3	0.3	43.08	16.18	Vis-Bisevo	L. byssoides	N/A	45	89	*
378	Z-4310	N/A	N/A	546	110	326	766	N/A	-0.70	0.30	0.3	0.3	43.08	16.18	Vis-Bisevo	L. byssoides	N/A	45	89	*
379	Z-4311	N/A	N/A	533	142	249	817	N/A	-0.70	0.30	0.3	0.3	43.08	16.18	Vis-Bisevo	L. byssoides	N/A	45	89	*
380	Z-4312	N/A	N/A	722	51	620	824	N/A	-0.70	0.30	0.3	0.3	43.08	16.18	Vis-Bisevo	L. byssoides	N/A	45	89	*
381	Z-4642	N/A	N/A	713	55	603	823	N/A	-0.70	0.30	0.3	0.3	43.08	16.18	Vis-Bisevo	L. byssoides	N/A	45	89	*
382	Z-4693	N/A	N/A	1342	64	1214	1470	N/A	-0.20	0.25	0.2	0.3	42.98	16.01	Vis-Bisevo	L. byssoides	N/A	45	89	*
383	Z-4694	N/A	N/A	1542	98	1346	1738	N/A	-0.20	0.25	0.2	0.3	42.98	16.01	Vis-Bisevo	L. byssoides	N/A	45	89	*
384	Z-4685	N/A	N/A	554	121	312	796	N/A	-0.70	0.30	0.3	0.3	42.98	16.01	Vis-Bisevo	L. byssoides	N/A	45	89	*
385	Z-4686	N/A	N/A	802	142	518	1086	N/A	-0.70	0.30	0.3	0.3	42.98	16.01	Vis-Bisevo	L. byssoides	N/A	45	89	*
386	Z-4692	N/A	N/A	-715	176	-1067	-363	N/A	-1.50	0.30	0.3	0.3	42.98	16.01	Vis-Bisevo	L. byssoides	N/A	45	89	*
387	Z-4695	N/A	N/A	1384	79	1226	1542	N/A	-0.20	0.25	0.2	0.3	43.01	16.22	Vis-Bisevo	L. byssoides	N/A	45	89	*
388	Z-4696	N/A	N/A	1372	72	1228	1516	N/A	-0.20	0.25	0.2	0.3	43.01	16.22	Vis-Bisevo	L. byssoides	N/A	45	89	*
389	GX-30414	N/A	N/A	-4014	211	-4436	-3592	N/A	-3.70	1.10	1.1	1.1	41.9	16.13	Battaglia lake	Charcoal	N/A	46	90	*
390	LTL-664A	N/A	N/A	-4860	132	-5124	-4596	N/A	-5.60	0.60	0.6	0.6	41.9	16.13	Battaglia lake	Seed	N/A	46	90	*
391	LTL-456A	N/A	N/A	-4999	206	-5411	-4587	N/A	-6.10	0.60	0.6	0.6	41.9	16.13	Battaglia lake	Seed	N/A	46	90	*
392	GX-24886	N/A	N/A	-1334	102	-1538	-1130	N/A	-1.00	1.00	1	1	41.57	15.84	Frattarolo lagoon	Plant remains	N/A	47	90	*
393	GX-30408	N/A	N/A	-1352	136	-1624	-1080	N/A	-1.60	0.30	0.3	0.3	41.57	15.84	Frattarolo lagoon	Sediment	N/A	47	91	*
394	UA-15675	N/A	N/A	-1448	168	-1784	-1112	N/A	-1.10	1.00	1	1	41.57	15.84	Frattarolo lagoon	Plant remains	N/A	47	92	*
395	UA-14598	N/A	N/A	-1460	196	-1852	-1068	N/A	-1.20	1.00	1	1	41.57	15.84	Frattarolo lagoon	Plant remains	N/A	47	92	*
396	LTL-2078A	N/A	N/A	-2467	160	-2787	-2147	N/A	-2.20	1.00	1	1	41.57	15.84	Frattarolo lagoon	Sediment	N/A	47	91	*
397	GX-28575	N/A	N/A	-3146	203	-3552	-2740	N/A	-2.50	1.00	1	1	41.57	15.84	Frattarolo lagoon	Shell	N/A	47	91	*
398	UA-13189	N/A	N/A	920	229	462	1378	N/A	-1.60	1.00	1	1	40.17	18.44	Alimini lake	Organics	N/A	48	93	*
399	UA-12577	N/A	N/A	-25	148	-321	271	N/A	-2.20	0.70	0.7	0.7	40.17	18.44	Alimini lake	Organics	N/A	48	93	*
400	UA-12578	N/A	N/A	-2120	174	-2468	-1772	N/A	-3.40	0.50	0.5	0.5	40.17	18.44	Alimini lake	Organics	N/A	48	93	*
401	UA-12054	N/A	N/A	-3512	144	-3800	-3224	N/A	-4.00	0.50	0.5	0.5	40.17	18.44	Alimini lake	Organics	N/A	48	93	*

References

1] Vacchi, M., Ghilardi, M., Melis, R. T., Spada, G., Giaime, M., Marriner, N., ... Rovere, A.New relative sea-level insights into the isostatic history of the Western Mediterranean. *Quaternary Science Reviews* **201**, 396-408 (2018).

2] Galassi, G., Spada, G. Sea-level rise in the Mediterranean Sea by 2050: Roles of terrestrial ice melt, steric effects and glacial isostatic adjustment. *Global and Planetary Change*, **123**, 55-66 (2014)

3] Peltier, W.R. Global glacial isostasy and the surface of the ice-age Earth: the ICE-5G (VM2) model and GRACE. *Annual Review of Earth and Planetary Sciences* **32**, 111-149 (2004).

4] Lambeck, K., Purcell, A. Sea-level change in the Mediterranean Sea since the LGM: model predictions for tectonically stable areas. *Quaternary Science Reviews* **24(18-19)**, 1969-1988 (2005).

5] Vacchi, M., Marriner, N., Morhange, C., Spada, G., Fontana, A., Rovere, A. Multiproxy assessment of Holocene relative sea-level changes in the western Mediterranean: Sea-level variability and improvements in the definition of the isostatic signal. *Earth-Science Reviews* **155,** 172-197 (2016).

6] Ferrer García. C., Blázquez Morilla. A. M. The evolution of the Albufereta lagoon (western Mediterranean): climate cycles and sea-level changes. *Journal of Coastal Research* **28(6),** 1617-1626 (2012).

7] Brisset. E., Burjachs. F., Navarro. B. J. B., de Pablo. J. F. L. Socio-ecological adaptation to Early-Holocene sea-level rise in the western Mediterranean. *Global & planetary change*, **169,** 156-167 (2018).

8] Dupré. M., Fumanal. M. P., Sanjaume. E., Santisteban. C., Usera. J. Quaternary evolution of Pego coastal lagoon (Southern Valencia. Spain). *Palaeogeography. Palaeoclimatology. Palaeoecology*. **68**, 291-299. (1988)

9] Ruiz. J. M., Carmona. P. La llanura deltaica de los ríos Júcar y Turia y la Albufera de Valencia. *Geomorfologia i Quaternari litoral*. Homenatge al Dr. V. Rosselló. 399-419 (2005).

10] Marco-Barba. J., Holmes. J. A., Mesquita-Joanes. F., Miracle. M. R. The influence of climate & sea-level change on the Holocene evolution of a Mediterranean coastal lagoon: Evidence from ostracod palaeoecology and geochemistry. *Geobios* **46(5)**. 409-421, 2013

11] Sanjaume. E., Segura. F., Garcia. M. L., Pardo. J. Recent sedimentation in Valencia Lagoon: preliminary results. *Journal of Coastal Research*, **8 (3),** 688-698, (1992)

12] Carmona-González. P. C., Ballester. J.P. 2011. Geomorphology. geoarchaeology & ancient settlement in the Valencian Gulf (Spain). *Méditerranée. Revue géographique des pays méditerranéens/Journal of Mediterranean geography*, **117**, 61-72, (2011),

13] Rodríguez-Pérez, A., Blázquez, A. M., Guillem, J., Usera, J. Maximum flood area during MIS 1 in the Almenara marshland (western Mediterranean): Benthic foraminifera and sedimentary record. *The Holocene*, **28(9)**, 1452-1466. (2018)

14] Carmona. P., Ruiz-Pérez. J. M. Blázquez. A. M., López-Belzunce. M., Riera. S..,Orengo. H. Environmental evolution and mid–late Holocene climate events in the Valencia lagoon (Mediterranean coast of Spain). *The Holocene*. **26(11)**. 1750-1765 (2016)

15] Blázquez. A. M., Rodríguez-Pérez. A., Torres. T., Ortiz. J. E. Evidence for Holocene sea level and climate change from Almenara marsh (western Mediterranean). *Quaternary Research* **88(2),** 206-222, (2017)

16] Giaime. M., Morhange. C., Ontiveros. M. Á. C., Fornós. J. J., Vacchi. M., Marriner. N. In search of Pollentia's southern harbour: Geoarchaeological evidence from the Bay of Alcúdia (Mallorca. Spain). *Palaeogeography. Palaeoclimatology. Palaeoecology*. **466**, 184-201, (2017)

17] Yll. R., Pantaleón-Cano. J., Pérez-Obiol. R.P., Roure. J. M. Cambio climático y transformación del medio durante el Holoceno en las Islas Baleares. Congrés del Neolític a la Península Ibérica. *Saguntum Extra***. 2**. 45-51, (1999).

18] Burjachs. F., Pérez-Obiol. R., Roure. J. M., Julià. R. Dinámica de la vegetación durante el Holoceno en la isla de Mallorca. *Trabajos de Palinología básica y aplicada*. 199-210, (1994).

19] Cearreta. A., Benito. X., Ibáñez. C., Trobajo. R., Giosan. L. Holocene palaeoenvironmental evolution of the Ebro Delta (Western Mediterranean Sea): Evidence for an early construction based on the benthic foraminiferal record. *The Holocene*. **26(9),** 1438-1456. (2016).

20] Riera-Mora. S. Esteban-Amat. A. Vegetation history and human activity during the last 6000 years on the central Catalan coast (northeastern Iberian Peninsula). *Vegetation History & Archaeobotany*. **3(1).** 7-23, (1994)

21] Daura. J. Sanz. M. Ramos. J. Riera. S., Miras. Y. Allué. E., Picornell-Gelabert. L., López-Reyes. D., Albert. R.M., Macià. L., Domènech. R., Martinell. J., Fornós. J.J., Julià. R. 2016. Palaeoenvironmental record of the Cal Maurici wetland sediment archive in Barcelona (NE Iberian Peninsula) between c. 6000 and 4000 cal. yr BP. *The Holocene*, **26(7)**. 1020-1039, (2016)

22] Ejarque. A., Julia. R., Reed. J. M., Mesquita-Joanes. F., Marco-Barba. J., Riera. S. Coastal evolution in a Mediterranean microtidal zone: Mid to Late Holocene natural dynamics & human management of the Castelló lagoon. NE Spain. *PloS one*. **11(5)**. e0155446, (2016).

23] Laborel. J., Morhange. C., Lafont. R., Le Campion. J., Laborel-Deguen. F., Sartoretto. S. Biological evidence of sea-level rise during the last 4500 years on the rocky coasts of continental southwestern France & Corsica. *Marine Geology* **120(3)**, 203-223, (1994)

24] Sabatier. P., Dezileau. L., Barbier. M., Raynal. O., Lofi. J., Briqueu. L., Condomines. M., Bouchette. F., Certain. R., Van Grafenstein. U. Jorda. C., Blanchemanche. P. (South of France). *Bulletin de la Societe Geologique de France* **181(1)**. 27-36, (2010).

25]Vella. C., Provansal. M. Relative sea-level rise and neotectonic events during the last 6500yr on the southern eastern Rhône delta. France. *Marine Geology* **170(1)** 27-39, (2000).

26] Amorosi. A. Rossi. V. Vella. C. Stepwise post-glacial transgression in the Rhône Delta area as revealed by high-resolution core data. *Palaeogeography. Palaeoclimatology. Palaeoecology* **374**, 314-326, (2013)

27] Morhange. C., Laborel. J., Hesnard. A. Changes of relative sea level during the past 5000 years in the ancient habour of Marseilles. Southern France. *Palaeogeography. Palaeoclimatology. Palaeoecology* **166(3)**, 319-329, (2001)

28] Vella. C., Fleury. T. J., Raccasi. G., Provansal. M., Sabatier. F., Bourcier. M. Evolution of the Rhône delta plain in the Holocene. *Marine Geology* **222**, 235-265, (2005)

29] Allinne. C., Devillers. B., Bertoncello. F., Bouby. L., Bruneton. H., Bui Thi. M., ... Revil. A. Archéologie et paléoenvironnement sur le site du pont romain des Esclapes (Fréjus. Var). *ArcheoSciences. Revue d'archéométrie*, **(30)**, 181-196, (2006)

30] Devillers. B., Excoffon. P., Morhange. C., Bonnet. S., Bertoncello. F. Relative sea-level changes and coastal evolution at Forum Julii (Fréjus. Provence). *Comptes Rendus Geoscience*, **339(5)**. 329-336, (2007)

31] Morhange. C., Marriner. N., Excoffon. P., Bonnet. S., Flaux. C., Zibrowius. H., Goiran. J. Amouri. M. E. Relative Sea-Level Changes During Roman Times in the Northwest Mediterranean: The 1st Century AD Fish Tank of Forum Julii. Fréjus. France. *Geoarchaeology* **28(4),** 363-372, (2013)

32] Colombaroli. D., Marchetto. A., Tinner. W. Long-term interactions between Mediterranean climate. vegetation and fire regime at Lago di Massaciuccoli (Tuscany. Italy). *Journal of Ecology*, **95(4)**, 755-770. (2007)

33] Carboni. M. G., Bergamin. L., Di Bella. L., Esu. D., Cerone. E. P., Antonioli. F., Verrubbi. V. Palaeoenvironmental reconstruction of late Quaternary foraminifera and molluscs from the ENEA borehole (Versilian plain. Tuscany. Italy). *Quaternary Research* **74(2)**, 265-276, (2010)

34] Kaniewski. D., Marriner. N., Morhange. C., Vacchi. M., Sarti. G., Rossi. V., Bini. M., Pasquinucci. M., Allinne. C., Otto. T. Luce. F., Holocene evolution of Portus Pisanus. the lost harbour of Pisa. Scientific reports, **8(1)**. *11625*, (2018)

35] Ghilardi. M., Istria. D., Curras. A., Vacchi. M., Contreras. D..,Vella. C., Dussouillez. P., Crest. Y., Guiter. F., Delanghe. D., Reconstructing the landscape evolution and the human occupation of the Lower Sagone River (Western Corsica. France) from the Bronze Age to the Medieval period. *Journal of Archaeological Science: Reports*, **12**, 741-754, (2017)

36] Ghilardi. M., Delanghe. D., Demory. F., Leandri. F., Pêche-Quilichini. K., Vacchi. M., Vella. M.A., Rossi. V., Robresco. S., Enregistrements d’événements extrêmes et évolution des paysages dans les basses vallées fluviales du Taravo et du Sagone (Corse occidentale. France) au cours de l'âge du Bronze moyen à final: une perspective géoarchéologique. *Géomorphologie: relief. processus. environnement*. **23(1)**. 15-35, 2017

37] Vacchi. M., Ghilardi. M., Spada. G., Currás. A., Robresco. S. New insights into the sea-level evolution in Corsica (NW Mediterranean) since the late Neolithic. *Journal of Archaeological Science: Reports* **12**, 782-793, (2017).

38] Poher. Y., Ponel. P., Médail. F., Andrieu-Ponel. V., Guiter. F. Holocene environmental history of a small Mediterranean isl& in response to sea-level changes. climate and human impact. *Palaeogeography. Palaeoclimatology. Palaeoecology*. **465** 247-263 2017.

39] Lambeck, K., Anzidei, M., Antonioli, F., Benini, A., Verrubbi, V. Tyrrhenian sea level at 2000 BP: evidence from Roman age fish tanks and their geological calibration. *Rendiconti Lincei. Scienze Fisiche e Naturali*, **29(1)**, 69-80 (2018)

40] Lambeck. K., Anzidei. M., Antonioli. F., Benini. A., Esposito. A. Sea level in Roman time in the Central Mediterranean and implications for recent change. *Earth and Planetary Science Letters* **224(3)**, 563-575, (2004)

41] Evelpidou. N., Pirazzoli. P., Vassilopoulos. A., Spada. G., Ruggieri. G., Tomasin. A. Late Holocene sea level reconstructions based on observations of Roman fish tanks. Tyrrhenian Coast of Italy. *Geoarchaeolog*y **27(3)**, 259-277, (2012)

42] Marra. F., Bozzano. F., Cinti. F. R. Chronostratigraphic and lithologic features of the Tiber River sediments (Rome. Italy): Implications on the post-glacial sea-level rise and Holocene climate. *Global and Planetary Change* **107**. 157-176, (2013)

43] Salomon. F. Géoarchéologie du delta du Tibre: évolution géomorphologique holocène et contraintes hydrosédimentaires dans le système Ostie-Portus (Italie). Thèse de doctorat en géographie. option géoarchéologie. soutenue en 2013 à l'Université Lumière Lyon 2. *Physio-Géo. Géographie physique et environnement*. **8** 1-6, (2014)

44] Goiran. J. P., Tronchère. H., Collalelli. U., Salomon. F., Djerbi. H. Découverte d'un niveau marin biologique sur les quais de Portus: le port antique de Rome. *Méditerranée* **1**, 59-67 (2009)

45] De Muro. S., Orrù. P. Il contributo delle Beach-Rock nello studio della risalita del mare olocenico. Le Beach-Rock post-glaciali della Sardegna nord-orientale. *Il Quaternario* **111**, 19-39, (1998)

46] Melis. R. T., Di Rita. F., French. C., Marriner. N., Montis. F., Serreli. G., Sulas. F., Vacchi. M. 8000 years of coastal changes on a western Mediterranean island: A multiproxy approach from the Posada plain of Sardinia. *Marine Geology* **403**, 93-108. (2018)

47] Melis. R. T., Depalmas. A., Di Rita. F., Montis. F., Vacchi. M. Mid to late Holocene environmental changes along the coast of western Sardinia (Mediterranean Sea). *Global and Planetary Change*, **155**, 29-41. (2017)

48] Di Rita. F., Melis. R.T. The cultural landscape near the ancient city of Tharros (central West Sardinia): vegetation changes and human impact. *Journal of Archaeological Science* **40(12)**, 4271-4282, (2013).

49] De Falco. G..,Antonioli. F., Fontolan. G., Lo Presti. V.. Simeone. S.. Tonielli. R. Early cementation and accommodation space dictate the evolution of an overstepping barrier system during the Holocene. *Marine Geology*, **369**, 52-66, (2015).

50] Ruiz, J. M., Carmona, P., Gómez-Bellard, C., van Dommelen, P. Geomorfología y cambio ambiental en el entorno de los yacimientos púnicos de la llanura de Terralba (Golfo de Oristano, isla de Cerdeña, Italia). *Boletín Geológico y Minero*, **129**, 331-52. (2018)

51] Orrù. P., Solinas. E., Puliga. G., Deiana. G. Palaeo-shorelines of the historic period. Sant'Antioco Island. south-western Sardinia (Italy). *Quaternary International* **232(1)**, 71-81, (2011)

52] Orrù. P. E., Mastronuzzi. G., Deiana. G., Pignatelli. C., Piscitelli. A., Solinas. E., Spanu. P., Zucca. R., Sea level changes and geoarchaeology between the bay of Capo Malfatano and Piscinnì Bay (SW Sardinia) in the last 4 kys. *Quaternary International* **336**, 180-189, (2014)

53] Orrù. P. E., Antonioli. F., Lambeck. K., Verrubbi. V. Holocene sea-level change in the Cagliari coastal plain (southern Sardinia. Italy). *Quaternaria Nova*, **8**, 193-212, (2004).

54] Barra. D., Romano. P., Santo. A., Campajola. L., Roca. V., Tuniz. C. The Versilian transgression in the Volturno river plain (Campania. Southern Italy): Palaeoenvironmental history and chronological data. *Il Quaternario,* **9(2)**, 445-458, (1996)

55] Sacchi. M., Molisso. F., Pacifico. A., Vigliotti. M., Sabbarese. C., Ruberti. D. Late-Holocene to recent evolution of Lake Patria. South Italy: An example of a coastal lagoon within a Mediterranean delta system. *Global and Planetary Change* **117**. 9-27, (2014).

56] Barra D.. Calderoni. G. Cipriani. M. De La Geniere' J.. Fiorillo. L. Greco. G. Mariotti Lippi M.. Depositional history and palaeogeographic reconstruction of Sele coastal plain during Magna Grecia settlement of Hera Argiva (Southern Italy). *Geologica Romana*, **35**, 151-166, (1999)

57] Amato. V., Aucelli. P. P. C., Ciampo. G., Cinque. A., Di Donato. V.. Pappone. G., ... Ermolli. E. R. Relative sea level changes and paleogeographical evolution of the southern Sele plain (Italy) during the Holocene. *Quaternary International* **288**, 112-128 (2013)

58] Barra. D. Calderoni G. Cinque A. De Vita P. Rosskopf CM. Ermolli ER. New data on the evolution of the Sele River coastal plain (southern Italy) during the Holocene. *Il Quaternario* **11**, 287–299, (1998)

59] Antonioli. F., Chemello. R., Improta. S., Riggio. S. The Dendropoma (Mollusca Gastropoda. Vermetidae) intertidal reef formations and their paleoclimatological use. *Marine Geology* **161**, 155-170, (1999)

60] Basso. D., Bernasconi. M. P., Robba. E., Marozzo. S. Environmental evolution of the Marsala sound. Sicily. during the last 6000 years. *Journal of Coastal Research*. **24(1)** , 177-197, (2008)

61] Spampinato. C. R., Costa. B., Di Stefano. A., Monaco. C., Scicchitano. G. 2011. The contribution of tectonics to relative sea-level change during the Holocene in coastal south-eastern Sicily: new data from boreholes. *Quaternary International* **232(1)**, 214-227, (2011)

62] Gerardi. F., Smedile. A..,Pirrotta. C., Barbano. M.S., De Martini. P.M., Pinzi. S., Gueli. A.M., Ristuccia. G.M., Stella. G., Troja. S.O. Geological record of tsunami inundations in Pantano Morghella (south-eastern Sicily) both from near and far-field sources. *Natural Hazards & Earth System Sciences* **12(4),** 1185-1200, (2012)

63] Marriner. N., Gambin. T., Djamali. M.. Morhange. C.. Spiteri. M. Geoarchaeology of the Burmarrad ria and early Holocene human impacts in western Malta. *Palaeogeography. Palaeoclimatology. Palaeoecology* **339**, 52-65 (2012)

64] Furlani. S.. Antonioli. F.. Gambin. T.. Biolchi. S.. Formosa. S.. Lo Presti. V.. ... Quarta. G. Submerged speleothem in Malta indicates tectonic stability throughout the Holocene. *The Holocene*. **28(10)**, 1588-1597. (2018).

65] Zaîbi. C., Carbonel. P., Kamoun. F., Azri. C., Kharroubi. A., Kallel. N., Jedoui. Y., Montacer. M., Fontugne. M. Évolution du trait de côte à l'Holocène supérieur dans la Sebkha El-Guettiate de Skhira (Golfe de Gabès. Tunisie) à travers sa faune d'ostracodes et de foraminifères. *Geobios* **44(1)**, 101-115. (2011)

66] Zaïbi, C., Carbonel, P., Kamoun, F., Fontugne, M., Azri, C., Jedoui, Y., Montacer, M. Evolution of the sebkha Dreîaa (South-Eastern Tunisia, Gulf of Gabes) during the Late Holocene: response of ostracod assemblages. *Revue de micropaléontologie*, ***55*(3)**, 83-97. (2012)

67] Morhange. C., Pirazzoli. P. A. Mid-Holocene emergence of southern Tunisian coasts. *Marine Geology* **220(1)**. 205-213. (2005)

68] Strasser. A., Davaud. E., Jedoui. Y. Carbonate cements in Holocene beachrock: example from Bahiret et Biban. southeastern Tunisia. *Sedimentary Geology* **62(1)**. 89-100. (1989)

69] Lakhdar. R., Soussi. M., Ben Ismail. M. H., M'Rabet. A. A Mediterranean Holocene restricted coastal lagoon under arid climate: Case of the sedimentary record of Sabkha Boujmel (SE Tunisia). *Palaeogeography. Palaeoclimatology. Palaeoecology* **241(2)**, 177-191. (2006)

70] Serandrei-Barbero. R., Albani. A., Donnici. S., Rizzetto. F. Past and recent sedimentation rates in the Lagoon of Venice (Northern Italy). *Estuarine, Coastal and Shelf Science* **69(1)**, 255-269, (2006)

71] McClennen. C.E., Housley. R.A. Late-Holocene channel meander migration & mudflat accumulation rates. lagoon of Venice, Italy. *Journal of Coastal Research* 930-945, (2006)

72] Zoppi. U., Albani. A., Ammerman. A. J., Hua. Q., Lawson. E. M. Barbero. R. S. Preliminary estimate of the reservoir age in the Lagoon of Venice. *Radiocarbon*, **43(2A)**, 489-494. (2001)

73] Madricardo, F., Donnici, S. Mapping past and recent landscape modifications in the Lagoon of Venice through geophysical surveys and historical maps. *Anthropocene* **6,** 86-96, (2014).

74] Tosi. L., Rizzetto. F., Bonardi. M., Donnici. S., Serandrei Barbero. R. Toffoletto. F. *Note illustrative della Carta Geologica alla scala 1: 50.000*. foglio **128** Venezia. APAT–Regione Veneto. 164 pp. (2007)

75] Donnici, S., Serandrei-Barbero, R., Canali, G. Evidence of climatic changes in the Venetian Coastal Plain (Northern Italy) during the last 40,000 years. *Sedimentary Geology* **281**, 139-150, (2012)

76] Galassi. P., Marocco. R. Relative sea level rise and subsidence in the Caorle Lagoon (Northern Adriatic Sea). Italy. during Holocene. *Il Quaternario*, **12**, 249-256, (1999)

77] Fontana. A., Vinci. G., Tasca. G., Mozzi. P., Vacchi. M., Bivi. G., ... Hajdas. I.. Lagoonal settlements and relative sea level during Bronze Age in Northern Adriatic: Geoarchaeological evidence & paleogeographic constraints. *Quaternary International* **439**, 17-36. (2017)

78] Fontana. A. Zanferrari. A., Foglio geologico 086" San Vito al Tagliamento" e Note Illustrative. *Carta geologica d'Italia alla scala 1: 50.000*. (2006)

79] Bondesan. A., Meneghel. M., Rosselli. R., Vitturi. A. Geomorphological Map of the Province of Venice. scale 1: 50.000. LAC. Firenze (4 sheets). (2004)

80] Furlani. S., Biolchi. S., Cucchi. F., Antonioli. F., Busetti. M., Melis. R. Tectonic effects on Late Holocene sea level changes in the Gulf of Trieste (NE Adriatic Sea. Italy). *Quaternary International* **232(1)**, 144-157, (2011)

81] Covelli. S., Fontolan. G., Faganeli. J., Ogrinc. N. Anthropogenic markers in the Holocene stratigraphic sequence of the Gulf of Trieste (northern Adriatic Sea). *Marine Geology*, **230(1-2)**, 29-51, (2006)

82] Melis. R., Furlani. S., Antonioli. F., Biolchi. S., Degrassi. V., Mezgec. K. Sea level and paleoenvironment during roman times inferred from coastal archaeological sites in Trieste (northern Italy). *Alpine and Mediterranean Quaternary*, **25(1)**, 41-55. (2012)

83] Ogorelec. B., Faganeli. J., Mišič. M., Čermelj. B. Reconstruction of paleoenvironment in the Bay of Koper (Gulf of Trieste. northern Adriatic). *Annales*, **11(187)**, e200. (1997)

84] Faivre. S., Fouache. E., Ghilardi. M., Antonioli. F., Furlani. S., Kovačić. V. Relative sea level change in western Istria (Croatia) during the last millennium. *Quaternary international*, **232(1-2)**, 132-143, (2011)

85] Cibin U. Stefani. M. Carta Geologica d'Italia alla scala 1:50.000. Foglio 187. Codigoro. Note illustrative. *Carta geologica d'Italia alla scala 1: 50.000*. (2009)

86] Correggiari. A., Roveri. M., Trincardi. F. Late Pleistocene andHolocene evolution of the north Adriatic Sea. *Il Quaternario* 9. 697-704, (1996).

87] Sarti. G., Centineo. M.C., Calabrese. L., Carta Geologica d'Italia alla scala 1:50.000. Foglio 205. Comacchio. Note illustrative. *Carta geologica d'Italia alla scala 1: 50.000*, (2009)

88] Marriner. N., Morhange. C., Faivre. S., Flaux. C., Vacchi. M., Miko. S., Rossi. I. R. Post-Roman sea-level changes on Pag Island (Adriatic Sea): Dating Croatia's "enigmatic" coastal notch? *Geomorphology* **221**, 83-94, (2014)

89] Faivre. S., Bakran-Petricioli. T., Horvatinčić. N., Sironić. A. Distinct phases of relative sea level changes in the central Adriatic during the last 1500years—influence of climatic variations?. *Palaeogeography. Palaeoclimatology. Palaeoecology* **369**, 163-174, (2013)

90] Caldara. M., Caroli. I., Simone. O. Holocene evolution and sea-level changes in the Battaglia basin area (eastern Gargano coast. Apulia. Italy). *Quaternary International* **183(1)**, 102-114. (2008)

91] Caldara. M., Simone. O. Coastal changes in the eastern Tavoliere Plain (Apulia. Italy) during the Late Holocene: Natural or anthropic? *Quaternary Science Reviews* **24(18)**, 2137-2145, (2005)

92] Di Rita, F., Simone, O., Caldara, M., Gehrels, W. R., Magri, D. Holocene environmental changes in the coastal Tavoliere Plain (Apulia, southern Italy): a multiproxy approach. *Palaeogeography, Palaeoclimatology, Palaeoecology*, **310(3-4)**, 139-151, (2011)

93] Primavera. M.. Simone. O.. Fiorentino. G.. Caldara. M. The palaeoenvironmental study of the Alimini Piccolo lake enables a reconstruction of Holocene sea-level changes in southeast Italy. *The Holocene* **21(4)**, 553-563. (2011)